DETERMINING THE LOCATION OF HYDRAULIC JUMP BY MODEL TEST AND HEC-2 FLOW ROUTING

A Thesis Presented to

The Faculty of the

Fritz J. and Dolores H. Russ
College of Engineering and Technology

Ohio University

In Partial Fulfillment

of the Requirement for the Degree

Master of Science

by

Chen-Feng Li

August, 1995

ACKNOWLEDGEMENTS

The author gratefully acknowledges the financial support from my family, advisor Dr. Chang (Civil Engineering Dept., Ohio University) and Feng Chia University (Taiwan). The author would like to thank the Civil Engineering Department for the help they provided by supplying the various equipment used for my studies. The author also wants to thank those who have helped in my thesis writing.

TABLE OF CONTENTS

LIST OF TABLES

LIST OF FIGURES

LIST OF SYMBOLS

A	Flow cross section area
A_m	The flow cross section area of the model
A_p	The flow cross section area of the prototype
a	A coefficient
a_1	Constant
a_2	Constant
b_1	Constant
b_2	Constant
C	A function of water depth, water volume, and channel slope (Eq. 4-6)
C'	A function of water depth, water volume, and channel slope (eq. 4-7)
c	Expansion or contraction loss coefficient
c_1	Constant
c_2	Constant
D	The depth of tailwater
D_1	The initial depth of water
D_2	The sequent depth of the water
D_h	The hydraulic depth
d_1	The initial depth of water
E	The specific energy of the flow
E_0	A specific energy for a given discharge

F	Froude No.
F_1	The initial Froude No.
F_2	The Froude No. downstream at section 2
ΣF_x	Result of external forces acting on the jump along the channel direction
g	Acceleration due to gravity
h	Hydrostatic head
h_1	The initial depth of water
h_b	Height of cubic roughness
h_e	The energy loss
h_L	Length of the jump
h_v	head of water velocity
k	A parameter
k_c	water conveyance
L	Dimension of length
L_j	Length of the jump
L_m	Length dimension of the model
L_p	Length dimension of the prototype
L_R	Length of the roughened bed
L_{re}	Linear scale ratio of the model to the prototype
L_s	The distance starting from the point of initial water depth (upstream) and ending at the beginning of the sill
L_w	Discharge-weighted reach length

M_1	The momentum rate per unit time upstream (before the jump)
M_2	The momentum rate per unit time downstream (after the jump)
ΔM	M_1-M_2
n	Manning roughness
p	Channel wetted perimeter
P_1	The hydrostatic pressure force upstream (before the jump)
P_2	The hydrostatic pressure force downstream (after the jump)
q	The flow discharge per unit width
q_m	The water discharge per unit width of the model
q_{max}	The maximum flow discharge per unit width
q_p	The water discharge per unit width of the prototype
q_{re}	The ratio of discharge per unit width of the model to the discharge per unit width of the prototype
R	Hydraulic radius
γ	The weight of water per unit volume
S	Height of the sill
S_f	Friction slope for channel reach
T	Top width of water surface
t	Time
v	The flow mean velocity in x-direction
v_0	The water mean velocity at flow cross section 0 before the sluice gate
v_1	The water mean velocity upstream (before the jump)

v_2	The water mean velocity downstream (after the jump)
v_{2m}	The water mean velocity downstream (after the jump)
v_m	The water mean velocity of the model
v_p	The water mean velocity of the prototype
v_{re}	The ratio of model velocity to the prototype velocity
V_v	Water volume within the jump
W	Weight of the water within the jump
ws_1	The water surface elevation upstream
ws_2	The water surface elevation downstream
x	The distance starting from the initial water depth along the channel bottom toward to the downstream
x_1	Constant
x_2	Constant
y	The flow depth
y_0	The water depth at flow cross section 0 before the sluice gate
y_1	The initial depth of water
y_{1ep}	The initial water depth of the prototype converted from the experimental data
y_{1m}	The initial water depth of the model
y_2	The sequent depth of water
y_{2ep}	The sequent water depth of the prototype converted from experimental data
y_{2m}	The sequent water depth of the model

y_{2tp}	The sequent water depth of the prototype converted from the Belanger eq.
y_m	The water depth of the model
y_p	The water depth of the prototype
Z	The height of the sill
Z_0	The channel bottom elevation at section 0
Z_1	The channel bottom elevation at section 1
ΔZ	Height of the drop
θ	slope of channel

CHAPTER I. INTRODUCTION

I.1 BACKGROUND OF STUDY

Interest in the hydraulic jump began to increase after the early 19th century. In 1828, Belanger connected the hydraulic jump with the Momentum Principle. Gibson (1913) did some experiments and the results gave the best verification of the Momentum Principle in the hydraulic jump. By way of general description, a hydraulic jump occurs when flow changes from supercritical to subcritical flow in a short distance. In other words, the flow depths change from low stage to high stage. Within a hydraulic jump, the flow is turbulent and dissipates a portion of the energy from the upstream high velocity flow. Presently, experts regard the hydraulic jump as the best way to dissipate energy of high velocity flow. For this reason, there are a lot of investigators at work on hydraulic jump analysis and many significant studies have been done. Because upstream high velocity is likely to cause serious erosion, many investigations of the hydraulic jump concentrate on two main purposes. One is how to prevent negative consequences in rivers or artificial hydraulic structures. The other is how to best use the hydraulic jump for energy dissipation without adverse effects.

In order to protect river channels or man-made hydraulic structures, hydraulic jumps act as an energy dissipator by reducing the upstream high flow velocity into low flow velocity to avoid serious scour or erosion. A hydraulic jump can serve several functions. It can raise

the tailwater head for resisting lift force of hydraulic structures such as dams, offer the best location for chemical mixting, or serve as a point where air is removed in an otherwise smoothly operating water transit system to improve the transmission.

I.2 PURPOSE OF STUDY

The main purpose of this research is to determine how to find out the location and length of the hydraulic jump in 1° through 5° slopes of rectangular channels. Dimensional analysis shows that the length of hydraulic jump is a function of the Froude Number and the sequent depth of the jump. Experiments in a laboratory channel model show a relationship between upstream flow Froude Number F_1 and the ratio of jump length and sequent depth after jump L_j/y_2. If the initial depth y_1 and F_1 are determined or measured, then the sequent depth and length can be determined. Furthermore, by using dynamic simulation to convert the model scale into a design channel scale, HEC-2 software can be used to locate the heel of a hydraulic jump. Because of the known length of the jump, the toe of the jump can be pinpointed.

I.3 BUCKINGHAM PI THEOREM AND DYNAMIC SIMULATION

The Buckingham Pi Theorem is a tool to provide the relationships between N quantities

with M dimensions. The quantities can be arranged as N-M independent dimensionless parameters. Therefore the functional relation must exist as

$$F(Q_1, Q_2, Q_2, \ldots, Q_n) = 0 \qquad (1\text{-}1)$$

where $Q_1, Q_2, Q_3, \ldots, Q_n$ are quantities and the representative dimensionless groupings $P_1, P_2, P_3, \ldots, P_m$ of quantities will construct the equation

$$f(P_1, P_2, P_3, \ldots, P_m) = 0 \qquad (1\text{-}2)$$

The next step is to choose a specific Froude Number F_1 for dynamic simulation to convert the laboratory model into a prototype or real channel.

I.4 EXPERIMENTS AND REQUIREMENTS

Because the Bernoulli energy equation and continuity equation are applied in this study to calculate the velocities before and after the sluice gate (upstream flow conditions), the following assumptions are necessary for upstream flow before the jumps:

1. The flow is a steady flow.
2. The flow is an incompressible flow.
3. The flow is a frictionless flow.
4. The flow is an irrotational flow.

The equipment in this experiment includes a channel with adjustable slopes, a water recycle system, a motor for controlling the water discharge, a sluice gate and tailwater sill combination to form a hydraulic jump and to controlling the head of tailwater, and a water container. The scale of the channel is 6 inches wide, 1 foot high and 8 feet long. The channel slopes can be adjusted from a range of -15° to 15°, see fig. 2. The channel slopes of these experiments were conducted with the channel tilted between 1° to 5° along its slope.

The sluice gate were controlled in different openings to ensure the hydraulic jumps were formed with different Froude numbers for each specific slope and flow discharge. For each specific channel slope, the sluice gate has 15 to 20 different openings. The results and a more detail analysis of the experiments will be described in following chapters.

1.5 THE FUTURE DEVELOPMENT OF THE STUDY

In the design of hydraulic structures, determining the location of a hydraulic jump is very important. As previously described, the hydraulic jump plays a critical role in fluid channels. For example, a chemical purification point should be constructed right before the toe of hydraulic jump. Therefore, a location of the jump should be determined first. In designing a stilling basin, the sequent depth of the jump should be known. The hydraulic jump can protect the banks of channels by slowing down the velocity of the continual high velocity flow to avoid scouring in a channel. In this study, experiments have been done to provide the

provide the figure showing the curves of relationships between a various L_j / y_2 and F_1. The HEC-2 model was involved to point out the locations of the toe and heel of the hydraulic jump. This approach presents a quick way to determine the location of the hydraulic jump.

CHAPTER II. LITERATURE REVIEW

II.1 THEORETICAL DEVELOPMENT OF THE HYDRAULIC JUMP

The theoretical development of the hydraulic jump has become popular in the early 19th century. The hydraulic jump is related to the momentum principle and numerous experiments have been conducted in the past in an attempt to quantify the hydraulic theory. Bidone (1818) first described the hydraulic jump in a small rectangular flume. The correct mathematical theory of the hydraulic jump was developed by Belanger (1828). Additional work on the relationship between the hydraulic jump and fluid momentum was carried out by Bresse (1860) and Unwin (1880) respectfully. Darcy and Bazin published the results from their experiments with the hydraulic jump in 1965. The first studies of the hydraulic jump in the US. was by Ferriday (1894). The theory of the hydraulic jump done by Safranez in 1929, in Germany, was verified by a series of two-dimensional experiments (Elevatorski, 1959). The U. S. Bureau Reclamation (1954) did a series of dimensionless analysis for the hydraulic jump (Chow, 1959).

II.2 STUDIES OF THE HYDRAULIC JUMP

The hydraulic jump is a practical subject in hydraulic engineering because the hydraulic

jump is regarded as the best way to dissipate energy present in a moving fluid. By using the hydraulic jump, the total energy of a moving fluid can be reduced which in turn prevents the fluid from scouring the channel banks. Also the hydraulic jump enables a portion of the fluid's kinetic energy to be converted which can stabilize downstream flow conditions. However, the theory of the hydraulic jump is not yet fully developed.

To date, there have been many researchers who have studied and written numerous papers about the hydraulic jump. In general the primary goal of studying the hydraulic jump is to improve channel designs by understanding the mechanics and dynamics of the fluid flow within the jump. To this end, researchers focus on a few specific features of the hydraulic jump. Bradley and Peterka (1957) investigated design of a stilling basin for a hydraulic jump. Chang (1988) devised a way to estimate the locations of hydraulic jumps. Rouse et.al (1959) inspected in the characteristics of different types of jumps. Ohtsu and Yasuda (1991) investigated the relationships among tailwater, upstream flow depth, and the Froude numbers at the upstream. Molinas et.al (1985) developed a computer model for the hydraulic jump. Rajaratnam and Ortiz (1977) worked on the behaviors of the jump in a drop down channel. Narayanan and Schizas (1980) presented the effect of sills on the hydraulic jump. Kindsvater (1944) observed the effects of a sloping channel on the hydraulic jump. Rhone (1977) studied the effects of channel bottom roughness on the jump. Wilson (1972) investigated the boundary layer effects in the hydraulic jump locations.

These topics can all be grouped into five main categories.

(1) Channel slopes and hydraulic jumps,
(2) Lengths and locations of the hydraulic jumps,
(3) Forces and the hydraulic jumps,
(4) Hydraulic structures and jumps,
(5) Computer simulation of hydraulic jump surface profiles.

Each of these categories will be described in detail in the following sections.

II.3 CHANNEL SLOPE AND THE HYDRAULIC JUMP

With respect to channel slope, the hydraulic jump can be grouped into two distinct categories: jump in horizontal channels and jumps in sloping channels. According to Chow (1959), as shown in Figure (2-1), jumps in a horizontal channel can be further classified into one of the following types:

1. Undular jump: $1 < F_1 < 1.7$ where F_1 = initial Froude number upstream.

   The undular jump is a very weak jump, and the water surface undulates up and down.

2. Weak jump: $1.7 < F_1 < 2.5$.

   A weak jump shows a series of rollers and eddies within the jump over the water's surface. Downstream the water flow remains nearly uniform. The energy loss is low in a weak jump.

3. Oscillating jump: $2.5 < F_1 < 4.5$.

An oscillating jump forms a large wave which can last for miles and makes an unlimited amount of erosion on channels with earth banks.

4. Steady jump: $4.5 < F_1 < 9$.

This jump is very steady because it is the least sensitive to tailwater conditions. There is no drastic oscillating wave and the water appears very steady. The steady jump may dissipate about 45% to 70% of the flow energy.

5. Strong jump: $F_1 > 9$.

The strong jump is characterized by a flow with remarkable rollers and extremely rough surface. A strong jump may reduce the energy about 85%. From the view of channel protection, a strong jump may be harmful.

The physical laws governing the hydraulic jump in a sloping channel are the same for the jump in a horizontal channel. The designer must consider the extra force on the water due to the acceleration of gravity in the hydraulic-jump body of water on the sloping channel when designing a sloping channel. For all cases, the apron arrangement desired should provide the greatest economy for the various discharges and tailwater conditions. In fact, there are few stilling basins built as horizontal aprons because the hydraulic jump would be very sensitive. A sloping channel has more merit than a horizontal channel. From the practical application view, the sloping channel is used not only to gain satisfactory operation over a wide range

of tailwater conditions but to also lower the cost of the construction.

The hydraulic jumps in a sloping channel can be classified into four distinct types, see Figure 2-2 and 2-3:

1. A-jump: The toe (the beginning) of an A-jump is located on the junction of the channel with different slopes, and the heel of the jump is on a the downstream reach of the channel. The A-jump occurs on the portion of the channel without crossing the junction of the complex channel in the downstream side.

2. B-jump: The B-jump develops from the steeper upstream reach of the channel, crosses the junction of the channel and then ends on the milder sloping channel at the downstream side.

3. C-jump: The C-jump starts on the upstream side of the channel with the steeper slope, and ends right at the junction of the complex channel.

4. D-jump: The D-jump begins on the upstream side of the channel where the channel slope is steeper and ends before crossing the junction of the complex channel.

In order to provide more information for improving the design conditions, Rajaratnam, and Murahari (1974) observed the flow characteristics of the jumps in sloping channels including

the mean flow patterns, velocity, pressure, shear distributions, fluctuation distribution and turbulent shear. The authors carried out their experiments with various slopes from 2% to 25%. The results of the experiments of the jumps by Rajaratnam showed that the turbulent mean velocity can be analyzed by using the model of the plane turbulent wall jet, since the distribution of velocity is similar. The bed shear in a sloping channel is larger than that of a level channel jump.

Ohtsu and Yasuda (1991) presented a series of equations showing the relationships among the jump length L_j to the sequent depth h_2 and slope θ for B-jump, and D-jump. The relationship between the conjugate depths h_1 and h_2 (the initial depth and sequent depth are called conjugate depths) were expressed as equations as well. The equations to show the locations of the jumps were presented in terms of h_1, h_2, and θ, see table (2-1).

II.4 LENGTH AND LOCATION OF THE HYDRAULIC JUMP

The length of a hydraulic jump is one subject of the studies described in the preceding sections. The length of the hydraulic jump, according to Elevatorski (1959), is defined as the distance from the point where water roller turbulence begins up to the point where no return flow is observable. This is very important when designing a stilling basin, since the length controls the size and the cost of the stilling basin. Presently, the length of the hydraulic jump cannot be determined from theoretical considerations alone. Some hydraulic researchers

constructed models to aid in their investigations of jump lengths.

Brandly and Peterka (1957) investigated length of the hydraulic jumps in a smooth rectangular channel and illustrated their results in a series of two dimensionless plots. The first plot showed the relationships between the ratio of the jump length, L_j, to the initial depth, y_1, before the jump and the Froude number. The second plot was the curve to show the relationships between the ratio of the jump length, L_j, to the tailwater depth, y_2, with respect to the Froude number. Fujita and Yasuda (1986) developed an equation for the length of a hydraulic jump:

$$L_j = a\,(h_1 * h_L)^{0.5} \qquad (2\text{-}1)$$

where:

a	=	a coefficient,
L_j	=	the length of the jump,
h_1	=	the initial depth of the jump,
h_L	=	the head loss within the jump.

Ali (1991) installed various roughnesses in a channel bottom to reduce the length of the jump, to lower the cost of the stilling basin design and to stabilize the jump action. In Ali's study, the following assumptions were made:

1. The channel is rectangular,
2. The flow is steady and incompressible,
3. The pressure distribution at two ends of the jump are hydro-static,
4. The velocity distribution before the jump is uniform.

The investigation of the dimensional analysis and experiments, yielded the following equation:

$$L_j / h_1 = K (F_1^2 - 1) \quad (2\text{-}2)$$

where:

K represents a parameter and a function of F_1.

The results show that $L_R / h_b = 28$ provides a significant reduction in the relative length of the jump L_j / h_1.

where:

h_b = the height of cubic roughness,
L_R = the length of the roughened bed.

For F_1 from 4 to 10, the range of the reduction is between 27.4% and 67.4%.

Hager (1992) examined the hydraulic jump free surface profiles, and developed an empirical equation to determine the length of the jump. These tests were carried out for various F_1, from 2 to10, in a sloping channel with rectangular cross sections. Based on numerous experiments, an equation is presented to express the relationship between the inflow depth h_1 and the length of the jump L_j:

$$L_j = h_1 * \{-12 + 160 \tanh (F_1 /20) \} \quad (2\text{-}3)$$

The jump location with respect to its length is another prospective subject of study. The location of the hydraulic jump plays an important role in practical engineering. Adam, et. al

(1993) investigated the characteristics of the B-jump with different toe locations, and introduced new expressions for the hydraulic quantities that govern a B-jump in three different slopes.

To prevent scouring and damage caused by high energy floodwater from the outlet of a reservoir, Chang (1988) applied the HEC-2 software and the Belanger equation (see equation 3-13) to estimate the location of the hydraulic jump for channels with varied slopes. Chang's study was based on a theoretical calculation method to approach the jump locations.

II.5 FORCES AND THE HYDRAULIC JUMP

The hydraulic jump is widely applied as an energy dissipator. The characteristics of the turbulent jump have been studied for decades. Rajaratnam (1965) and Rouse (1959) published studies about the mean flow and turbulent characteristics of the hydraulic jumps. Narayanan (1975,1980) and McCorqyadale and Khalifa (1980) worked on theoretical analyses of the mean flow within the hydraulic jump and provided more information about how the jump exerts its forces on the hydraulic structures and how to designing hydraulic structures.

Narayanan and Shazis (1980) wrote their papers: " Force Fluctuations On Sill Of Hydraulic Jump " and " Force On Sill Of Forced Hydraulic Jump" to address the problem

of damage to the spillway of a dam from the pressure fluctuations of hydraulic jump and spillway current. More recently, Toso and Bowers (1988) studied the large pressure fluctuation in hydraulic-jump stilling basins. The fluctuation pressures are the pressures that act on the hydraulic structures or water channels caused by oscillating flow waves. The author quoted Elder's (1961) study to explain that the gravity and inertia forces dominate low-frequency fluctuation pressure while the high-frequency fluctuation pressures are cause from the turbulence associated with viscous forces.

The tests by Toso and Browers were conducted with Froude numbers from 3 to 10, and chute slopes of 0°, 15°, 30°, and 45°. The study indicated the fluctuation pressures are a function of the Froude number, the distance from the toe of the jump, and the boundary layer development. The investigators observed:

1. The practical upper limit of pressure magnitudes were reached in the duration of 12 to 24 hours.
2. The maximum pressure fluctuations on the floor usually happen at about one-third of the distance through the jump.
3. The longitudinal scale of extreme pressure pulses in the zone of maximum turbulence is eight times the incident flow depth.
4. The fluctuation pressure head in the jump tend to approach 80%-100% of the entering velocity head.
5. Whether or not the inflow is fully developed has little effect on the fluctuation

pressure.

6. Whether the channel bottom has blocks, sills or neither does not make much difference in fluctuation pressure.
7. The sidewall fluctuation pressure head's peak is about one to two inflow depths above the floor.

Farhoudi and Narayanan (1991) investigated the characteristics of the fluctuation. They concluded that the intensity of force fluctuations on an area of slab beneath a jump vary with respect to the jump area's length, the channel width, and the distance from the toe of the jump.

II.6 HYDRAULIC STRUCTURES AND JUMPS.

A hydraulic jump may occur in natural ways, but for practical purposes the hydraulic jump can also be created by man-made hydraulic structures. A hydraulic jump for a channel can be controlled or be formed by different hydraulic constructions such as a sluice gate upstream and a sill downstream. A jump is usually confined partly or entirely to a stilling basin. These constructions will be discussed in following sections.

II.6.1 HYDRAULIC JUMPS IN STILLING BASINS.

For a spillway, sluice gates are placed upstream and sills are placed downstream of stilling basins. Frank (1969) investigated the fluctuating pressure caused by the hydraulic jump. The investigators emphasized that the jump dissipates the flow energy and causes severe pressure fluctuations, and so should be considered in the design of a stilling basin. Narayanan (1980) claimed that a jump in a stilling basin will cause severe fluctuation pressure and cavitation is likely to happen.

Brandly and Peterka (1957) provided a simple method to design a dependable stilling basin with dimensionless forms for basin characteristics. One hundred and twenty five tests were conducted in Brandly's experiments. There are at least four different distinct forms of the jumps occurring in horizontal aprons:

1. Pre jump (F_1 = 1.7-2.5) - very low energy loss,
2. Transition (F_1 = 2.5-4.5) - rough water surface,
3. Good jumps (F_1 = 4.5-9) - least affected by tailwater variations,
4. Effective jumps ($F_1 > 9$) - effective but rough.

II.6.2 SLUICE GATES AND HYDRAULIC JUMPS.

A sluice gate is a very common hydraulic structure to force the flow into supercritical flow conditions. By changing the opening of the sluice gate, the water surface elevation before the gate and the water pressure head can increase. This change causes the velocity of flow

after the gate to become a supercritical flow if the pressure head of water increment is large enough. When designing such gates, the hydraulic engineer is mostly interested in the head-discharge relationship and the pressure distribution over the gate surface for various positions of the gate and forms of the gate lips.

In order to use the mathematical method to estimate the contraction coefficients and water surface profile configurations, Larock (1969) published his study examining the flow contraction coefficients and water surface profiles after the sluice gate. The author made these assumptions: the flow is steady, two-dimensional, irrotational, and incompressible. Usually the contraction coefficient measured from the field is larger than the theoretical one. Larock considered that this phenomenon is caused by the boundary effects. Rajaratnam (1977) published his study investigating free flow immediately below a sluice gate in a rectangular channel. The experiments by Rajaratnam are concerned on the characteristics of the discharges after the sluice gate and then dealt with the contraction coefficients. The author also drew conclusions from experimental investigations dealing with the water surface profile and its similar properties and the pressure field in the supercritical stream below the gate. Ohtsu and Yasuda (1994) observed the boundary layer affecting the jump after the sluice gate moving the jump location to various tailwater levels in the horizontal apron. The results of this study showed that the drag force on the vertical sill of a forced jump for the undeveloped supercritical flow is larger than that for the fully developed supercritical flow.

II.6.3 SILLS AND THE HYDRAULIC JUMP

Sills are another type of typical downstream structural controller. The hydraulic jump can be formed or effected by sills of various design, such as sharp-crested weirs, board-crested weirs, or abrupt rises and drops. The functions of sills are to ensure the formation of a jump and to control its position under all probable operating conditions. Weaver (1950) presented that the forces acting on the sills decrease rapidly to minimum as the end of the jump is moved upstream to a position approximately over the sill. The forces then increase slowly to a constant value as the jump is moved further upstream. The hydraulic research based on the theoretical analysis cannot fully provide an accurate knowledge of the hydraulic jump forced by sills. Most investigations focused on either the mathematical approximations of the flow or on its engineering applications.

Rand (1965) published a paper describing flow over a vertical sill in an open channel. The author emphasized that practical engineering applications are handicapped if either the relationship between the recommended design and the physical appearance of the flow is not comprehended or if one cannot predict the changes in the flow pattern of design modification. In order to obtain more accepted design methods and flexible design principles, a model to examine the complex flow phenomena was built with a moveable apron and an adjustable tailwater controlling gate which minimized the error of the measurements.

The experimental data was arranged as two sets of dimensionless parameters with the

relationships between the dimensionless parameters. The first set was with a curve expressing the relationship between the ratio of D_2 / D_1 (D_1 : the depth before the jump and D_2 : the depth after jump), and the ratio S / D_1 (S : the height of sills) for specific Froude numbers. The second set was the relationship shown as a curve for D / D_1 and L / D_1 (D : the depth of the tailwater, and L : length of the natural hydraulic jump). This study provided an empirical equation to interpret the parameter L_s / D_1 (L_s : the distances from the depths before the jumps to sills) :

$$L_s / D_1 = \min (L_s / D_1) + k (\max L_s / D_1 - \min L_s / D_1) \quad (2\text{-}4)$$

$$k = \{ (L_s / D_1) - \min (L_s / D_1) \} / \{ (\max L_s / D_1 - \min L_s / D_1) \} \quad (2\text{-}5)$$

and the energy loss distributes in three main regions with various k :

1. The energy loss within the jump upstream of the sill,
2. The energy loss under the bottom after sill,
3. The surface rollers downstream of the sill.

The results of the experiments by Rand show that the largest total energy loss will happen when the k = 0 for different Froude numbers, and k increases the rate of energy dissipation decreases with distance.

Karki, et al. (1972) examined the incipient phenomena of the hydraulic jump of a flow

over a sill in an open channel to study jump prediction and jump stabilization. The investigators operated the experiments with low discharges and low Froude numbers in order to reach incipient jump flow conditions. The experiment showed that if the ratio of Z / d_1, (Z = the height of the sill, and the d_1 = the depth before the sill where flow starts to rise) is greater than 1.25 the water jet does not splashing-over. If the ratio of Z / d_1 is less than 1.25, the water jet will separate. Karki's experiments indicated that the Z / d_1 ratio increases with the upstream Froude number F_1. There is little change in the drag coefficient when the F_1 is greater than 2.3.

Hager, et. al (1986) presented their study on the incipient jump condition for ventilated sill flow in rectangular channel. The experiments were carried out in a channel with a drop after the sill, and a sill on a horizontal channel. Hager's study was based on the longitudinal momentum theorem, and tried to predict the limitation of the relative sill height S (the ratio of sill's height s to the water depth d_1 without rise before sill) without calculating gravity flow jumps in terms of approaching F_1. Hager and Li (1992) examined a sill-controlled energy dissipator. The author inspected the effects of a continuous, transverse sill on the hydraulic jump of a rectangular channel with two- and three-dimensional flows.

Besides sluice gates and sills, an abrupt drop downstream can provide the additional depth for the hydraulic jump. The drop will stabilize the formation of the hydraulic jump. Moore and Morgan (1957) investigated the characteristics of an abrupt drop in a channel bottom and found that two different forms of the jump may occur. One jump occurs before the drop and

the other after the drop. The results (Moore et.al., 1957) showed that if the jump forms at upstream of the drop the hydrostatic pressure (r h) has a maximum value:

$$r\,h = r\,y_2 \tag{2-6}$$

where:

h = the hydrostatic head,
r = the weight of water per unit volume,
y_2 = the water depth after jump.

If the jump forms at downstream of the drop, the hydrostatic pressure (r h) has a minimum value:

$$r\,h < (\Delta z + y_1) \tag{2-7}$$

where:

Δz = the height of drop,
y_1 = the depth before jump.

Sharp (1974) presented a study about the effects of the channel drop on the hydraulic jump. Sharp focused on a jump where large waves occurred on the channel with a drop. Because this jump wave could raise the tailwater and may exceed 50% of the original tailwater depth, the investigator attempted to determine whether it would be possible to design a step inhibiting wave formation. The formation of large standing waves can be greatly

inhibited or eliminated by rounding the edge of the abrupt step. The results (Sharp, 1974) showed that the maximum and minimum tailwater depths are generally less than those which would be obtained from theoretical considerations alone. The author also found that the lower tailwater depths can be controlled better than higher tailwater depths by rounding the edge of step drop.

Rajaratnam and Ortiz (1977) presented more information about the hydraulic jump and waves at abrupt drops. The author carried out the experiments with various initial Froude numbers F_1, from 3.14 to 10.55, and relative drop height h / y_1 (here h is the drop height, and y_1 is the initial depth) from 1.26 to 5.68. The A- jumps and B-jumps were discussed in this study. If the upstream flow has a supercritical flow condition and the tailwater level is too high at downstream A-jump will occur. A B-jump will occur if the tailwater level is reduced to a suitable depth. Hager (1985) investigated the B-jumps at abrupt channel drops. The differences in water surface profiles between A-jump and B-jump were discussed in Hager's study. According to Hager's study, the water surface profile was an upward curve if the jump was an A-jump and the water surface profile was a downward curve if the jump was a B-jump. The properties of effective pressure distribution and the internal flow process of the B-jump in a rectangular channel with channel drop were examined. A more accurate relationship for the conjugate flow depths was presented.

II.7 COMPUTER SIMULATION OF HYDRAULIC JUMP SURFACE PROFILES

The water surface profile of the hydraulic jump is associated with the conjugate depths, initial depth and sequent depth. The depth before the jump is called initial depth, and the depth after the jump is called sequent depth. The hydraulic experts have investigated this subject for decades. The ratio of the conjugate depths is the first computation needed to analyze water surface profile. Only for the case of an open channel with a rectangular cross section is it possible to solve for this ratio directly. For other cross sections, the equations giving the ratio of the conjugate depths are implicit and require that the solution be produced by trail and error, or by an iterative procedure. Jeppson (1970) provided a quick graphic method to obtain the ratio of conjugate depths.

Several methods have been used to determine the water surface profiles, the most common of which are the DIRECT STEP METHOD and the STANDARD STEP METHOD. As known, the computation processes of these method are based on trial and error or iteration. Because there is no easy way to determine the water surface within the jump, some hydraulic experts have worked intensely to solve this problem. Rajaratnam and Subramanya (1968) investigated the profiles of the jumps and developed a generalized profile for the hydraulic jump in smooth and rectangular channels, by use of bed pressure and water-surface profiles.

With the improvement of computers, the complex calculation problems for water surfaces do not exist at all. In the 1960's the HEC-2 program was developed to compute the water

surface profile. Since it is based on the energy concept, this software can not be directly used to compute the water surface profile where the energy changes rapidly. Although the limitation exists, Chang (1988) presented a method to find the heel of the jump by applying the Belanger equation and performing a subcritical routine of HEC-2 program.

Martin and DeFazio (1969) published their study of applying a digital computer to simulate the open-channel surge. The definition of surge here is a gravity wave generated by sudden or rapid variation. In a river, a flood wave surge, or on ocean wave possessing severe water-surface profile variations produce a breaking front, commonly called a bore or a moving hydraulic jump. In order to estimate the water surface for wave problems in prismatic open-channel , the authors applied the equations of motion for gradually-varied flow in finite difference form. The equation arises from the applicability of gradually varied flow theory to problems involving surges or rapidly-varied wave forms.

Most of the computer programs were designed for water surface profile calculations on gradually varied open channel flows by applying the energy concept to construct the mathematical equations. Molinas and Yang (1985) introduced a new method which uses both energy and momentum equations to compute the water surface profiles. The authors announced that their program can be used to estimate the water surface profiles of the jump in various channel slopes.

Gharangik and Chaudry (1991) used the continuity and momentum equations as the

governing equations for one-dimension and unsteady open-channel flow to build a numerical simulation model of the hydraulic jump while the boundary conditions have been given.

$$\frac{\partial q}{\partial x} + \frac{\partial y}{\partial t} = 0 \qquad (2\text{-}8)$$

$$\frac{\partial(v\, y)}{\partial t} + \frac{\partial}{\partial x} [\, y\, v^2 + (0.5)\, g\, y^2 - \frac{y^3}{3} (\frac{\partial^2 v}{\partial x\, \partial t} + v \frac{\partial^2 v}{\partial x^2}) - (\frac{\partial v}{\partial x})^2] = 0 \qquad (2\text{-}9)$$

where:

t = time,
x = the distance along the channel bottom toward to the downstream,
v = the flow velocity in x-direction,
y = the flow depth,
g = acceleration due to gravity.

Gharangik's (1991) study provided another technique to estimate the locations of the hydraulic jump in the laboratory. Robinson and McGhee (1993) developed a computer model for side weirs. Unlike the Araz's model, the authors claimed that their model can be used for supercritical, subcritical, or the combination of both flow conditions in declining-flow regimes without boundary conditions. Also, if the hydraulic jump occurs in the flow, the location of the jump can be determined.

θ (1)	D-jump: $0° < \theta \leqq 19°$ (2)	B-Jump	
		$0° < \theta \leqq 19°$ (3)	$19° < \theta \leqq 60°$ (4)
Length of jump	$L_j/h_2 = 5.75 \tan\theta + 5.70$ $(4 \leqq F_1 \leqq 14)$	$L_j/h_2 = 5.75 \tan\theta + 5.70$ $(4 \leqq F_1 \leqq 14)$	$L_j/h_2 = 4.6(h_d/h_2 - 1) + 5.7$ $(4 \leqq F_1 \leqq 14)$
Momentum equation	$(h_1/d_1)^3 - [k(L_j/d_1)(1/\cos\theta + h_1/d_1)\tan\theta + \tan^2\theta + 2F_1^2 + 1](h_1/d_1) + 2F_1^2 \cos\theta = 0$ where $k = 1 + 10^{-(2.8\tan\theta + 0.74)}$	$(h_d/d_1)^3 - [k'(l/d_1)(1/\cos\theta + h_j/d_1)\tan\theta + 2F_1^2 + 1 + \tan^2\theta + k'(1 - r)(h_j/d_1 + h_d/d_1)(L_j/d_1 - l/d_1)\tan\theta](h_d/d_1) + 2F_1^2 \cos\theta = 0$ where $h_j/d_1 = [1/\cos\theta + (l/d_1)\tan\theta] + [h_d/d_1 - (l/d_1)\tan\theta - 1/\cos\theta](l/d_1)/(L_j/d_1)$ and $r = 1 + 10^{-[(0.64 + 0.49/\tan\theta)h_d/h_2 + 0.1]}$ and $k' = 1 + 10^{-(2.8\tan\theta + 0.74)}$	$(h_d/d_1)^3 - [k'(l/d_1)(1/\cos\theta + h_j/d_1)\tan\theta + 2F_1^2 + 1 + \tan^2\theta + k'(1 - r)(h_j/d_1 + h_d/d_1)(L_j/d_1 - l/d_1)\tan\theta](h_d/d_1) + 2F_1^2 \cos\theta = 0$ where $h_j/d_1 = [1/\cos\theta + (l/d_1)\tan\theta] + [h_d/d_1 - (l/d_1)\tan\theta - 1/\cos\theta](l/d_1)/(L_j/d_1)$ and $r = 1 + 10^{-[(0.64 + 0.49/\tan\theta)h_d/h_2 + 0.1]}$ and $k' = 1 + 10^{-(2.8\tan\theta + 0.74)}$
Sequent depths	$h_1/d_1 = (0.077\theta^{1.27} + 1.41)(F_1 - 1) + 1$ (θ in degree) $(4 \leqq F_1 \leqq 14)$	$l/h_2 = [2.3/(\tan\theta)^{0.75} - 0.8](h_d/h_2 - 1)^{0.75}$ $(6 \leqq F_1 \leqq 14,\ 1.1 \leqq h_d/h_2 \leqq 3.0)$	$l/h_2 = [2.3/(\tan\theta)^{0.75} - 0.8](h_d/h_2 - 1)^{0.75}$ $(6 \leqq F_1 \leqq 14,\ 1.1 \leqq h_d/h_2 \leqq 3.0)$

Table 2-1: Relationship of the Hydraulic quantities for D- and B-jumps (by Iwao Ohtsu et. al., 1991)

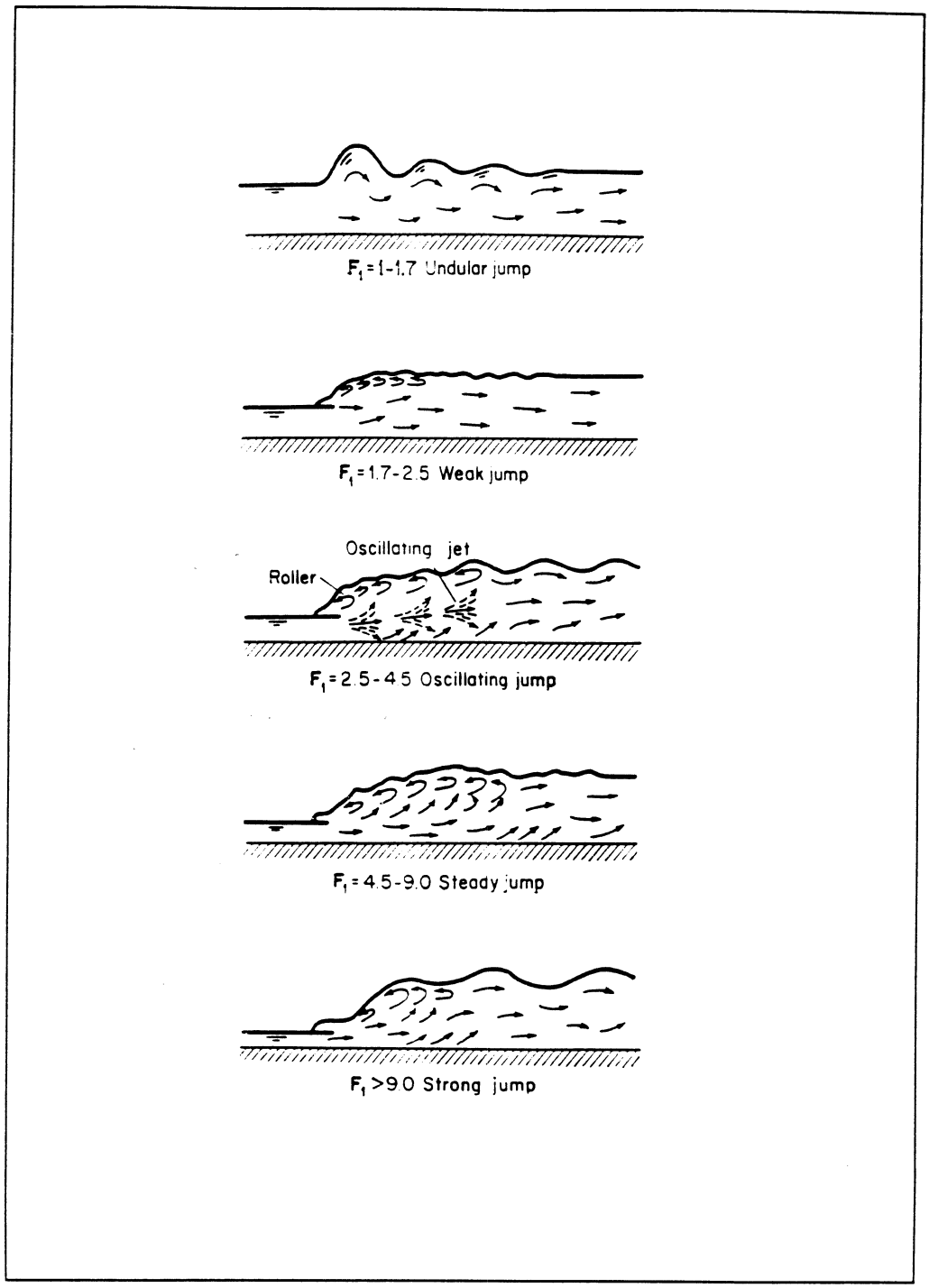

Figure 2-1: types of the hydraulic jumps in horizontal channels (OPEN-CHANNEL HYDRAULICS,Chow, 1959)

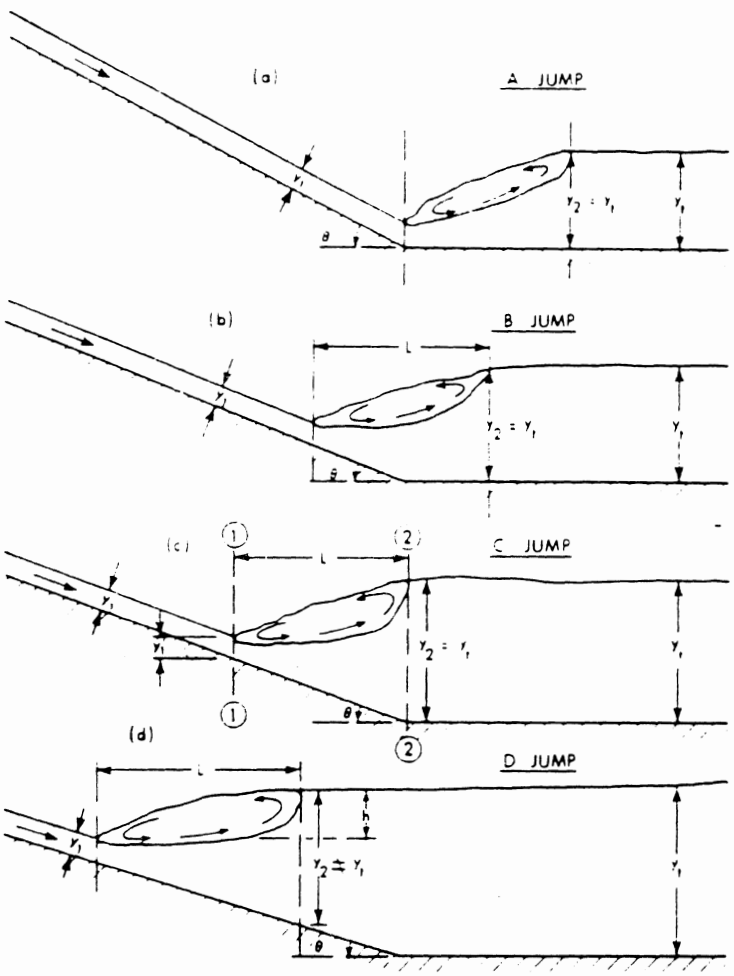

Figure 2-2: types of the hydraulic jumps in sloping channels
(by Nallamuthu Rajaratnam et. al., 1974)

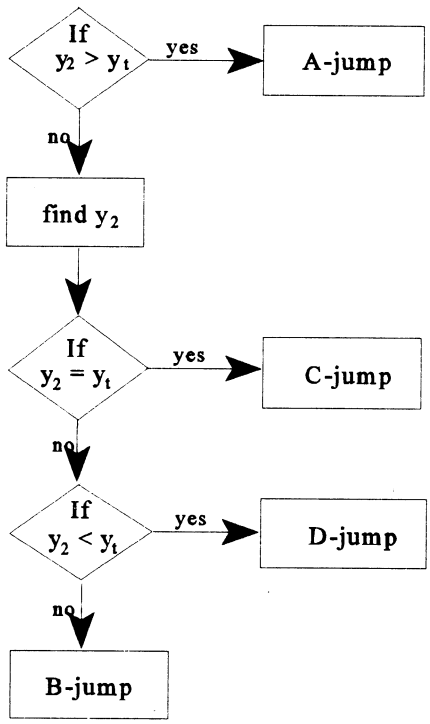

where: y_2 is the sequent depth after the jump
y_t is the tailwater depth

Figure 2-3: classification of the jump in sloping channel

CHAPTER III. METHODOLOGY AND EXPERIMENTS

III.1 FLOW CONDITIONS AND HYDRAULIC JUMPS

Water flow in a open channel can be classified into three different types: supercritical flow, critical flow and subcritical flow, as given in Figure 3-1. To form a hydraulic jump, the flow must be in a supercritical flow at the upstream side and end with subcritical flow region at the downstream side. Different flow conditions have different engineering applications. For example, a hydraulic engineer may have to deal with supercritical flows for a spillway design and subcritical flows for a reduction of channel bank scouring.

III.1.1 FLOW CONDITIONS

A subcritical flow is defined as having a Froude number less than one. In this case, the velocity of the flow is lower than the gravity wave velocity, i.e. a low velocity head and high pressure head. On the other hand, a supercritical flow is defined as having a Froude number greater than one. A supercritical flow has a velocity greater than the wave velocity at a given the flow depth. The supercritical flow could damage the river banks with high velocity scouring. However, the supercritical flow has a higher velocity head, which may be useful for application needing a high kinetic energy, such as rotating a turbine in a hydroplant.

The critical flow is the condition in which the Froude number is equal to one, or a flow with a specific energy is minimum for a given discharge. The critical flow can be obtained by a delicate balance of several conditions: the flow velocity equals half of the hydraulic depth D (D= flow cross section A divided by top width of water surface T), as given in Figures 3-2 and 3-3. For a rectangular cross section of a horizontal channel, the hydraulic depth is equal to the water depth (y = D). When

$$E = y + \frac{v^2}{2g} = y + \frac{q^2}{2gy^2} \quad , \tag{3-1}$$

To find the condition of the minimum energy we differentiate the Equation 3-1 by letting dE/dy = 0. The result can be written as

$$\frac{v^2}{2g} = \frac{y}{2} \quad , \tag{3-2}$$

where:

E = the specific energy of channel flow,
v = the mean velocity of channel flow,
q = the flow discharge per unit width.

To determine how q varies with y for a given $E = E_0$ is important. As given in Figure 3-3,

graphing the E-q curve of Equation 3-1 shows that when $y \doteq E_0$, $v \doteq 0$, which implies $q \doteq 0$. Similarly, when $y \doteq 0$, then $q \doteq 0$. This gives a flow value depth, y, corresponding to a value of E with $q = q_{max}$. Rewriting Equation 3-1 as

$$q^2 = 2 g y^2 (E_0 - y) \quad , \tag{3-3}$$

differentiating with respect to y and letting dq/dy equal 0, the equation becomes

$$2 q \frac{d q}{d y} = 4 g y E_0 - 6 g y^2 = 0 \quad , \tag{3-4}$$

$$y = \frac{2}{3} E_0 \tag{3-5}$$

The above equations result in that $y = 2/3\ E_0$, which corresponds to $q = q_{max}$ as shown in Figure 3-3.

III.1.2 BASIC CONCEPTS OF THE HYDRAULIC JUMPS

Theoretically, the total momentum flux is equal to the total external forces exerted on the control volume for both the supercritical flow before a hydraulic jump and the subcritical

flow after the hydraulic jump, i.e., the change of momentum per unit time between the beginning and the end of a hydraulic jump must equal the total force exerted on the moving water mass within the jump. The following assumptions are made:

1. The channel is rectangular in shape and the width of the channel sides do not change,
2. The friction loss within the hydraulic jump is negligible,
3. The streamline concept is still used between the two ends of the hydraulic jump,

As shown in Figure 3-4, the momentum equation can be expressed as the following equation,

$$P_1 - P_2 = M_2 - M_1 \qquad (3\text{-}6)$$

where:

P_1, P_2 represent the hydrostatic forces acting on sections 1 and 2, respectively,

M_1, M_2 represent the flow momentum flux at sections 1 and 2, respectively.

III.2 THE BASIC THEORY OF THIS STUDY

In this study, a model was built to simulate the real channel. The dimensional analysis is used to analyze possible variables involved in the study of a hydraulic jump.

III.2.1 DIMENSIONAL ANALYSIS

The function of dimensional analysis is to deal with problems due to complex variables in a model test. Dimensional analysis is a popular method for planning an experimental model study. It is convenient to do the dimensional analysis to rearrange the key variables into dimensionless terms, which simplifies the problem and enables the creation of a model. A good performance of dimensional analysis can provide a proper direction for a model study before money and time are blindly wasted. Thanks to the dimensional analysis, complex variables can be reduced into simple dimensionless terms that make an analytic solution of a difficult problem possible.

III.2.2 THE APPLICATION OF DIMENSIONAL ANALYSIS

In this study, the Buckingham PI theorem was used to analyze hydraulic parameters involved in a hydraulic jump as following :

L_j = the length of the hydraulic jump,
g = the acceleration due to gravity,
y_1 = the initial depth of the jump upstream,
y_2 = the sequent depth of the jump downstream,
v_1 = the mean velocity of upstream section.

The functional relationship of $F(L_j, g, y_1, y_2, v_1) = 0$ must exist. Choosing v_1 and y_2 as repeating variables, we have:

$$\Pi_1 = v_1^{a_1} y_2^{a_2} L_j = \left(\frac{L}{T}\right)^{a_1} L^{a_2} L^1 \quad , \tag{3-7}$$

$$\Pi_2 = v_1^{b_1} y_2^{b_2} g = \left(\frac{L}{T}\right)^{b_1} L^{b_2} \left(\frac{L}{T^2}\right)^1 \quad , \tag{3-8}$$

$$\Pi_3 = v_1^{c_1} y_2^{c_2} y_1 = \left(\frac{L}{T}\right)^{c_1} L^{c_2} L_1 \quad , \tag{3-9}$$

where:

a_1, a_2, b_1, b_2, c_1, c_2 represent constants,
L represents the dimension of length,
T represents the dimension of time.

These dimensionless terms can be arranged into

$$\Pi_1 = \frac{L_j}{y_2} \quad , \tag{3-10}$$

$$\Pi_2 = g \frac{y_2}{v_1^2} \quad , \tag{3-11}$$

$$\Pi_3 = \frac{y_1}{y_2} \quad , \tag{3-12}$$

where π_2 can be rewritten as $\pi_2 = f(F_1)$. According to the Belanger equation

$$\frac{y_2}{y_1} = \frac{1}{2}\left(\sqrt{1 + 8F_1^2} - 1\right), \tag{3-13}$$

and π_3 is a function of F_1. Therefore the relationship between these quantities can be expressed by

$$F = f\left(F_1, \frac{L_J}{y_2}\right) \tag{3-14}$$

Equation 3-14 from the dimensional analysis shows that the Froude number,F_1, and L_j/y_2 can be used to describe the flow behavior in a hydraulic jump. The experiments of this study are based on these two dimensionless terms and are conducted in differently sloped channel bottoms. Since the interest of this study is the length of the hydraulic jump, L_j, Equation 3-15 is rearranged into

$$\frac{L_J}{y_2} = f(F_1) \tag{3-15}$$

III.3 EXPERIMENTS OF HYDRAULIC JUMPS

Based on the results of the dimensional analysis, the experiments can be directed towards the relationships between the ratio of the length of the hydraulic jump to the sequent depth,

L_j/y_2, and the Froude number of the upstream flow, F_1. The laboratory model for these experiments, given in Figure 3-5, includes an adjustable channel 8 feet long, 6 inches wide and 1 foot deep. With a proper adjustment of discharge control valve, sluice gate and tailwater sill, a hydraulic jump can be formed in the channel.

The experiments were conducted on varied channel bed slopes from 1^0 through 5^0. As shown in Figure 3-6 and Table 3-1 to 3-5, four variables measured in the experiments are

1. The water depth, y_0, at the channel section before sluice gate (at section 0),
2. The water depth y_1 of upstream flow before the hydraulic jump (at section 1),
3. The water depth at the end of jump y_2 (at section 2),
4. The jump length L_j .

By applying the continuity principle of Equation 3-16 and Bernoulli theory of Equation 3-17,

$$v_0 y_0 = v_1 y_1 \quad , \tag{3-16}$$

$$z_0 + \frac{v_0^2}{2g} + y_0 = z_1 + \frac{v_1^2}{2g} + y_1 \quad , \tag{3-17}$$

the mean velocity at section 0 can be calculated by Equation 3-18

$$v_0 = \left[2g \frac{(y_0 - y_1 + \Delta z)}{(y_0 / y_1)^2 - 1} \right]^{1/2} , \qquad (3\text{-}18)$$

where: Δz is the elevation difference between section 0 and section 1, $(z_0\text{-}z_1)$.

After v_0 is obtained, rewriting Equation 3-16 as

$$v_1 = v_0 \frac{y_0}{y_1} , \qquad (3\text{-}19)$$

the mean flow velocity v_1 can be determined by Equation 3-19. The Froude number, F_1, can be computed by the following equation:

$$F_1 = \frac{v_1}{\sqrt{g\, y_1}} \qquad (3\text{-}20)$$

The purpose of the experiments was to build the relationship between two dimensionless terms F_1 and the ratio L_j/y_2, and will be discussed in Chapter 4.

Similarly, the mean velocity of the downstream flow, v_2, can also be estimated by the continuity equation, i.e., $v_2 = v_1 (y_1 / y_2)$. Thereby, the Froude number, F_2, can be computed by the following equation:

$$F_2 = \frac{v_2}{\sqrt{g\, y_2}} \qquad (3\text{-}21)$$

After F_2 is determined, the mean flow velocity, v_2, and the water depth, y_2, are measured. These will be used to estimate mean flow velocity, v_{2p}, in the corresponding prototype channel by applying the dynamic similitude concept. The model y_2 is also used to estimate y_{2p} for the prototype to simulate the prototype water surface calculation by the HEC-2 software program.

III.4 DYNAMIC SIMULATION

There are specific relationships between a model and its corresponding prototype hydraulic structure. The dynamic simulation serves as an aid to demonstrate these relationships between models and prototype hydraulic structures. Hydraulic engineers have established laboratory models to help their studies and apply dynamic simulations to convert the discharge of the flow, the size of the sluice gate, the depth of the flow or the velocity of the models' flows into those of actual hydraulic structures. The application of dynamic simulation in engineering not only helps hydraulic structure design but also lowers the cost of building the structure.

After the dimensional analysis, the dynamic similarity is introduced to convert the scales

of the laboratory models into those of corresponding prototypes. Since an open channel flow is mainly governed by the gravity, the Froude number is the key element for the flow phenomenon. Given flow conditions, the Froude number is kept the same for both the model and the prototype flows. Based on the dynamic simulation, the velocity of the prototype is calculable by Equation 3-22

$$F = \frac{v_m}{\sqrt{g\, y_m}} = \frac{v_p}{\sqrt{g\, y_p}} \tag{3-22}$$

where:

F = Froude number,
v_m = the flow mean velocity of the model,
v_p = the flow mean velocity of the prototype,
g = the acceleration due to gravity,
y_m = the flow depth of the model,
y_p = the flow depth of the prototype.

If all homologous dimensions are equal between a model and a prototype, the following equations exist:

$$L_{re} = \frac{L_m}{L_p} \quad , \tag{3-23}$$

$$v_{re} = \frac{v_m}{v_p} = (L_{re})^{1/2} \quad , \tag{3-24}$$

$$q_{re} = \frac{q_m}{q_p} = (L_{re})^{3/2} \quad , \tag{3-25}$$

where:

L_{re} = linear scale ratio of the model to the prototype dimension,
L_m = length dimension of the model,
L_p = length dimension of the prototype,
v_m = the mean velocity of the model,
v_p = the mean velocity of prototype,
v_{re} = the ratio of the model velocity to the prototype velocity,
q_m = the flow discharge per unit width of the cross section of the model,
q_p = the flow discharge per unit width of the cross section of the prototype,
q_{re} = the unit width discharge ratio of the model to the prototype.

Rearranging Equation 3-22, the flow mean velocity, v_p, can be determined by Equation 3-26

$$v_p = v_m \sqrt{\frac{y_p}{y_m}} \tag{3-26}$$

For a given water depth, y_m, of the model, the flow cross section area, A_p, can be estimated

by

$$A_p = \frac{A_m}{A_{re}} = \frac{A_m}{(L_{re})^2} \quad , \tag{3-27}$$

where:

A_p = the cross section area of the flow of the prototype.
A_m = the cross section area of the flow of the model.

If the unit width discharge is used, it can be expressed by Equation 3-28

$$q_p = \frac{q_m}{L_{re}^{3/2}} \tag{3-28}$$

The water depth of the prototype, y_p, can be obtained by Equation 3-29

$$y_p = L_{re} \frac{q_p}{v_p} = \frac{y_m}{L_{re}} \tag{3-29}$$

Using the processes described above we can calculate the prototype sequent depths.

III.5 DETERMINATION OF PROTOTYPE SEQUENT DEPTHS

In this study, there are two ways to determine the sequent depth for a hydraulic jump. These are done by using the sequent depth directly converted from y_{2m}, a measurement by model test, and by applying Equation 3-13, respectively.

III.5.1 SEQUENT DEPTH AND DIRECT MODEL CONVERSION

To convert measured sequent depths in the model to obtain the prototype sequent depths, the continuity equation was applied. Substituting y_2 and v_2 into Equation 3-16, the continuity equation can be rewritten as

$$v_{2m} = \frac{y_{1m}}{y_{2m}} v_{1m} \quad , \tag{3-30}$$

where:

y_{1m} = the initial depth of the model at section 1, see Figure 3-6,
v_{1m} = the mean flow velocity of the model at section 1,
y_{2m} = the sequent depth measured of the model at section 2,
v_{2m} = the mean flow velocity of the model at section 2.

After v_{2m} was determined, F_2 can be calculated by using Equation 3-22 and rewriting equation 3-22 as

$$F_2 = \frac{v_{2\,m}}{\sqrt{g\ y_{2\,m}}} = \frac{v_{2\,ep}}{\sqrt{g\ y_{2\,ep}}} \quad , \tag{3-31}$$

where:

v_{2ep} = the mean flow velocity of the prototype channel at section 2 converted from experiment data,
y_{2ep} = the sequent flow depth of the prototype estimated from the model,
g = the acceleration of gravity.

By Equations 3-26, 3-30 and 3-31, y_{2ep} can be estimated by

$$y_{2\,ep} = \frac{y_{2\,m}}{L_{re}} \quad , \tag{3-32}$$

where:

y_{2ep} = the flow sequent depth.

III.5.2 SEQUENT DEPTH AND BELANGER EQUATION

Using Equation 3-13 to determine the sequent depth for the prototype flow, the upstream Froude number, F_1, is calculated first by Equation 3-20. When F_1 is obtained, the initial upstream water depth, y_{1ep}, can be determined from the model by using Equation 3-33

$$y_{1ep} = \frac{y_{1m}}{L_{re}} \quad , \tag{3-33}$$

where:

y_{1ep} = the initial water depth converted from experimental data.

After y_{1ep} was determined, the sequent water depth of the prototype is calculated by

$$y_{2tp} = y_{1eP} \times \frac{1}{2} \left(-1 + \sqrt{1 + 8 F_1^2} \right) \quad , \tag{3-34}$$

where:

y_{2tp} = the sequent depth of the prototype calculated by the Belanger equation of Equation 3-34.

III.6 HEC-2 FLOW ROUTING AND HYDRAULIC JUMP

The HEC-2 software programs are based on the one dimensional energy equation to computate the water surface profiles (HEC-2 Manual), by using the standard step method. HEC-2 uses the following two equations:

$$h_e = L_w \bar{s}_f + c \left| \frac{v_2^2}{2g} + \frac{v_1^2}{2g} \right| \quad , \tag{3-35}$$

$$ws_2 + \frac{v_2^2}{2g} = ws_1 + \frac{v_1^2}{2g} + h_e \quad , \tag{3-36}$$

where:

ws_1 and ws_2 = the water surface elevations at each reach ends,
v_1 and v_2 = the mean velocities at the ends of the reaches,
g = gravitational acceleration,
h_e = energy head loss,
L = discharge-weighted reach length,
s_f = representative friction slope for channel reach,
c = expansion or contraction loss coefficient.

The computation procedure (HEC-2 Manual) is as follows:

1. The user gives a specific water surface elevation at the downstream section for a subcritical flow computation, or a specific water surface elevation at the upstream section for a supercritical flow.
2. According to the given water surface elevation, the corresponding total conveyance, k_c, and the velocity head, h_v, are calculated by

$$k_c = \frac{1.486}{n} A R^{2/3} \quad , \tag{3-37}$$

where:

n = Manning roughness,

$$h_v = \frac{v^2}{2g} \tag{3-38}$$

A = the cross sectional area of the reach,
R = the hydraulic radius = A/p,
p = the wetted perimeter,
v = the mean flow velocity of the reach cross-section.

3. The s_f and h_e are computed by employing the value from the step 2,
4. The ws_2 is calculated by using the values from step 3,
5. The computed value of ws_2 and the ws_2 given in step 1 are compared and steps 1 through 5 are repeated until the difference between the two values of ws_2 are within a given accuracy.

III.7 DETERMINING THE LOCATION OF HYDRAULIC JUMP.

The standard step method for computing the water surface profile of gradually varied flow is based on the energy principle. The energy changes significantly within a hydraulic jump, therefore HEC-2 alone cannot be used to compute the water surface profile when a hydraulic jump occurs in the flow. Realizing this limitation of the HEC-2 program, this study incorporates experimental results of the model test in the HEC-2 flow routing to estimate the

location of the jump heel.

III.7.1 LOCATION OF JUMP HEEL

The HEC-2 program can perform both subcritical and supercritical flow calculations. When running subcritical flows, the value of the tailwater surface elevation has to be known for the program to proceed the computation of the water surface profile from the downstream to upstream end. There is a corresponding water depth value computed by HEC-2 equal to the value of sequent water depth estimated by either Equation 3-32 or 3-34 . The cross section in which the flow depth is the same as the sequent depth during the HEC-2 flow routing is the heel of the hydraulic jump.

The procedure of the HEC-2 flow routing for determining the heel of a hydraulic jump is illustrated in the following example:

1. A 1000 meters long , 10 meters wide, and 20 meters deep channel with a unit width discharge 16.4 (cms/m) is used.
2. Given a tailwater depth of prototype for the HEC-2 subcritical flow routing, the 1000 meters channel is divided into 10 reaches with 100 meters per reach.
3. Perform the HEC-2 subcritical flow routing.
4. Compare the calculated results from the routing with the sequent depth of prototype, y_{2ep}, estimated from the experimental test, and identify the reach in which y_{2ep} is located.

5. Divide the identified reach into finer reaches, i.e. less than 100 m. Execute the HEC-2 subcritical flow routing again.
6. Locate the jump heel by repeating steps 1 to 5 until a satisfactory result is obtained.

III.7.2 LOCATIONS OF JUMP TOE

Chang (1988) used the HEC-2 program to determine the location of the jump heel, where the location of the jump toe was defined as the section immediately preceding the heel of the jump. This study uses a different way to locate the toe of the jump by applying a constructed relation between the jump length ratio, L_j/y_2, and the Froude number F_1, i.e., Equation 3-15 from the experiment. Given the upstream Froude number F_1, the corresponding ratio of L_j/y_2 was obtained from the experimental relation. Because the ratio L_j/y_2 is a dimensionless parameter, the length of hydraulic jump, L_j, can be computed by the ratio multiplied by the converted prototype sequent depth, y_{2ep}. The distance is measured from the point of the jump heel toward the upstream end and ends at the distance equal to the value of L_j. The cross section of the end of the distance L_j is the toe of the hydraulic jump.

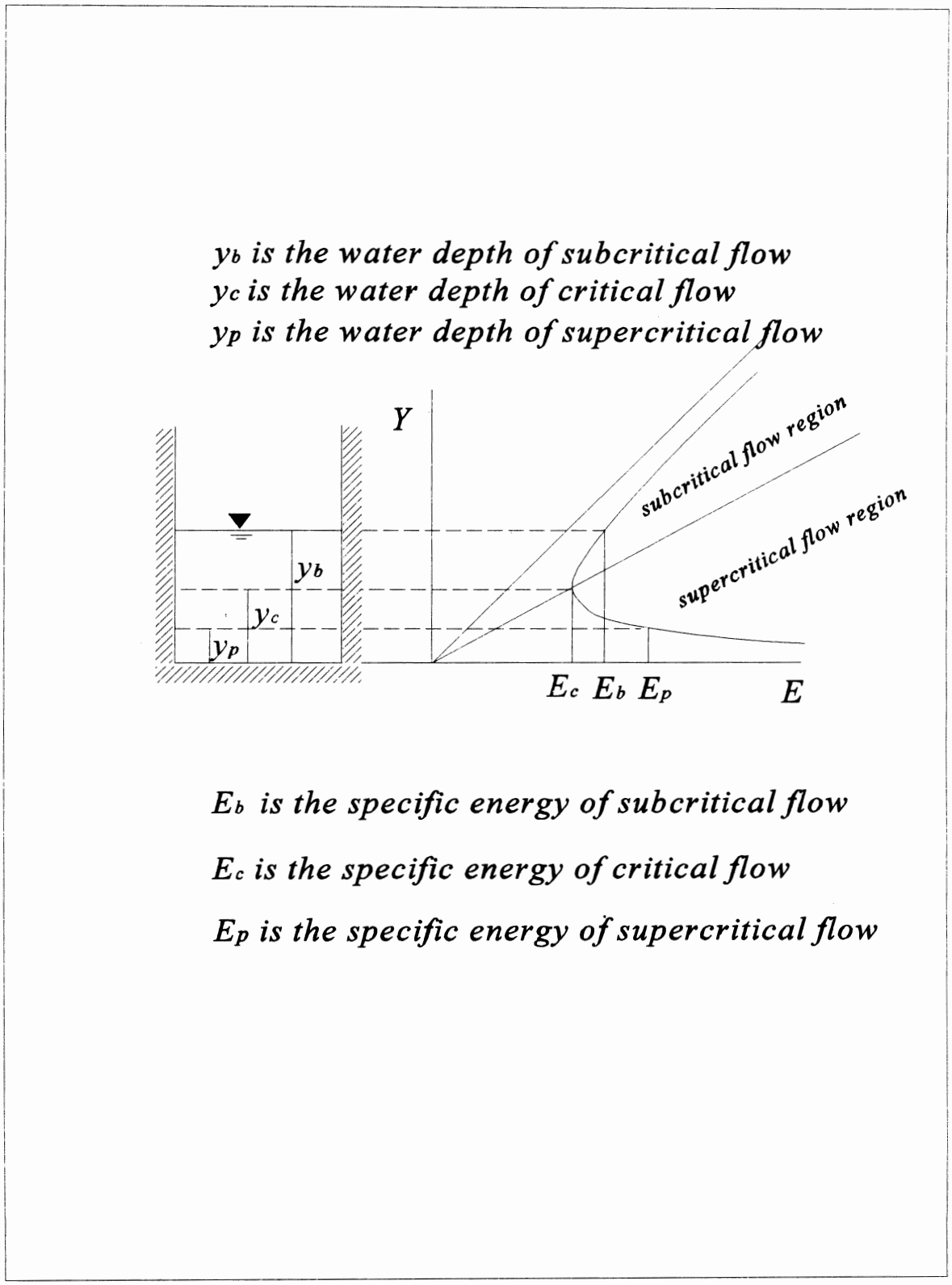

Figure 3-1: The characteristics of different flow conditions

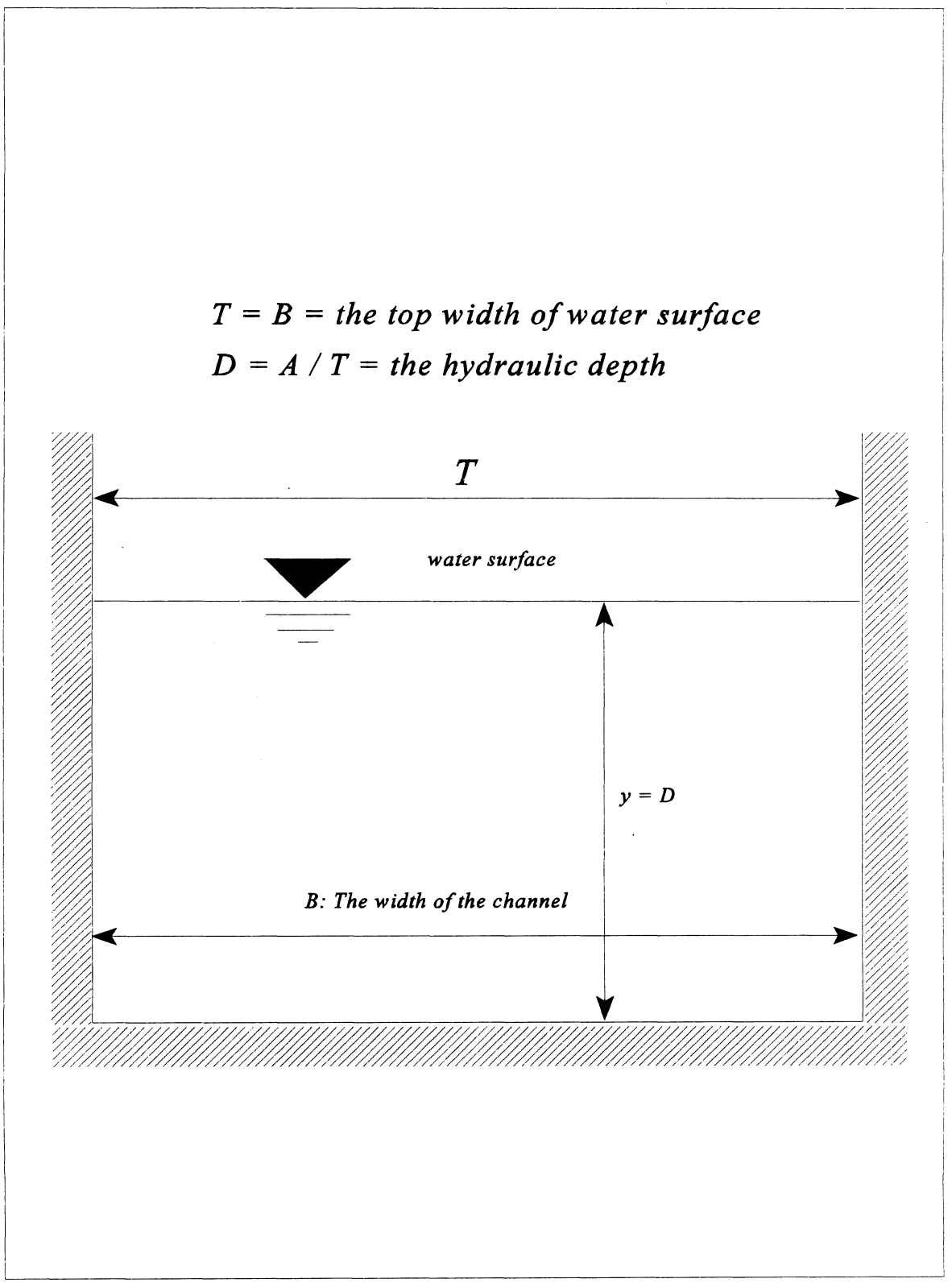

Figure 3-2: The illustration of a rectangular flow cross section

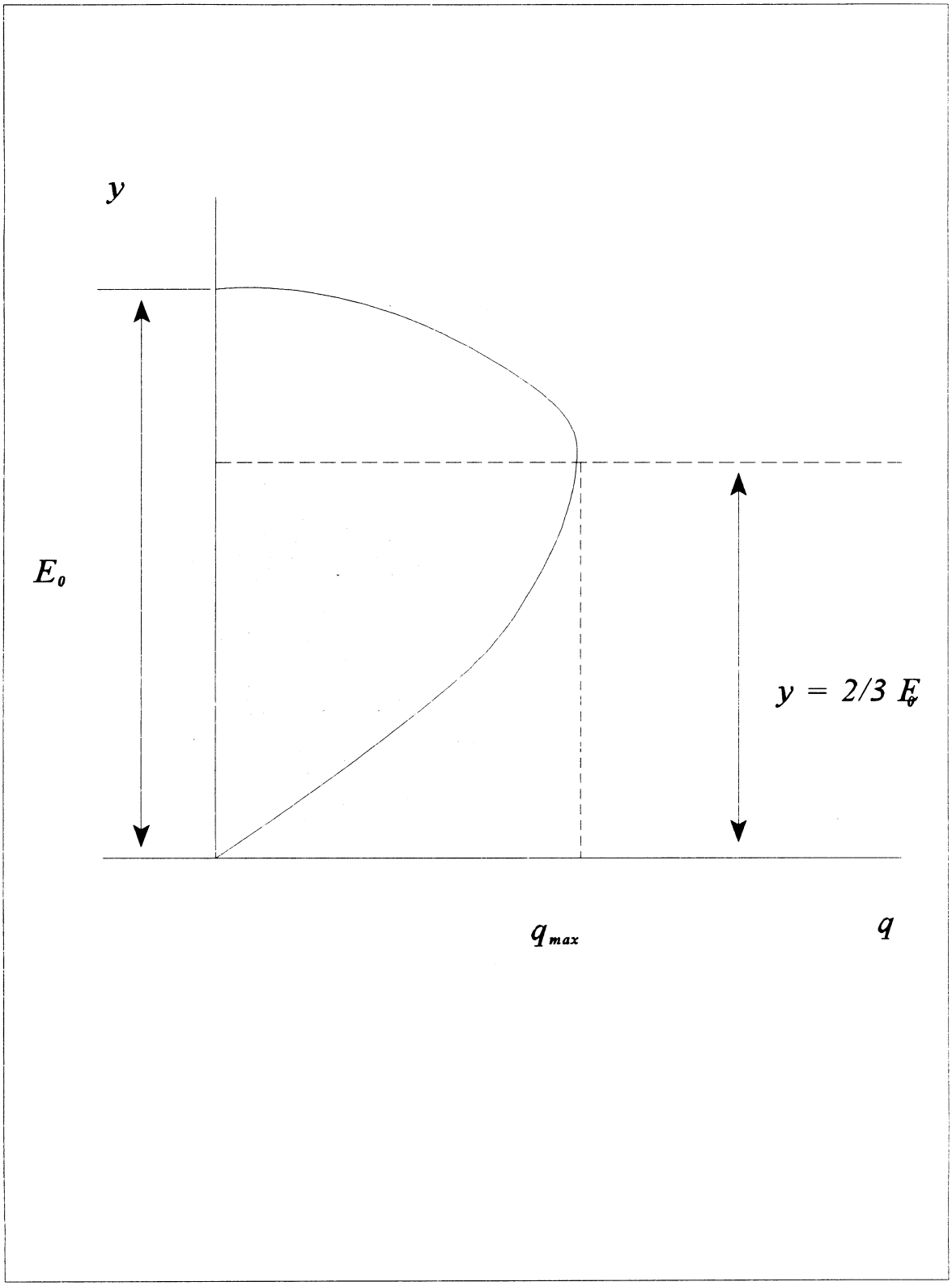

Figure 3-3: The E-q curve

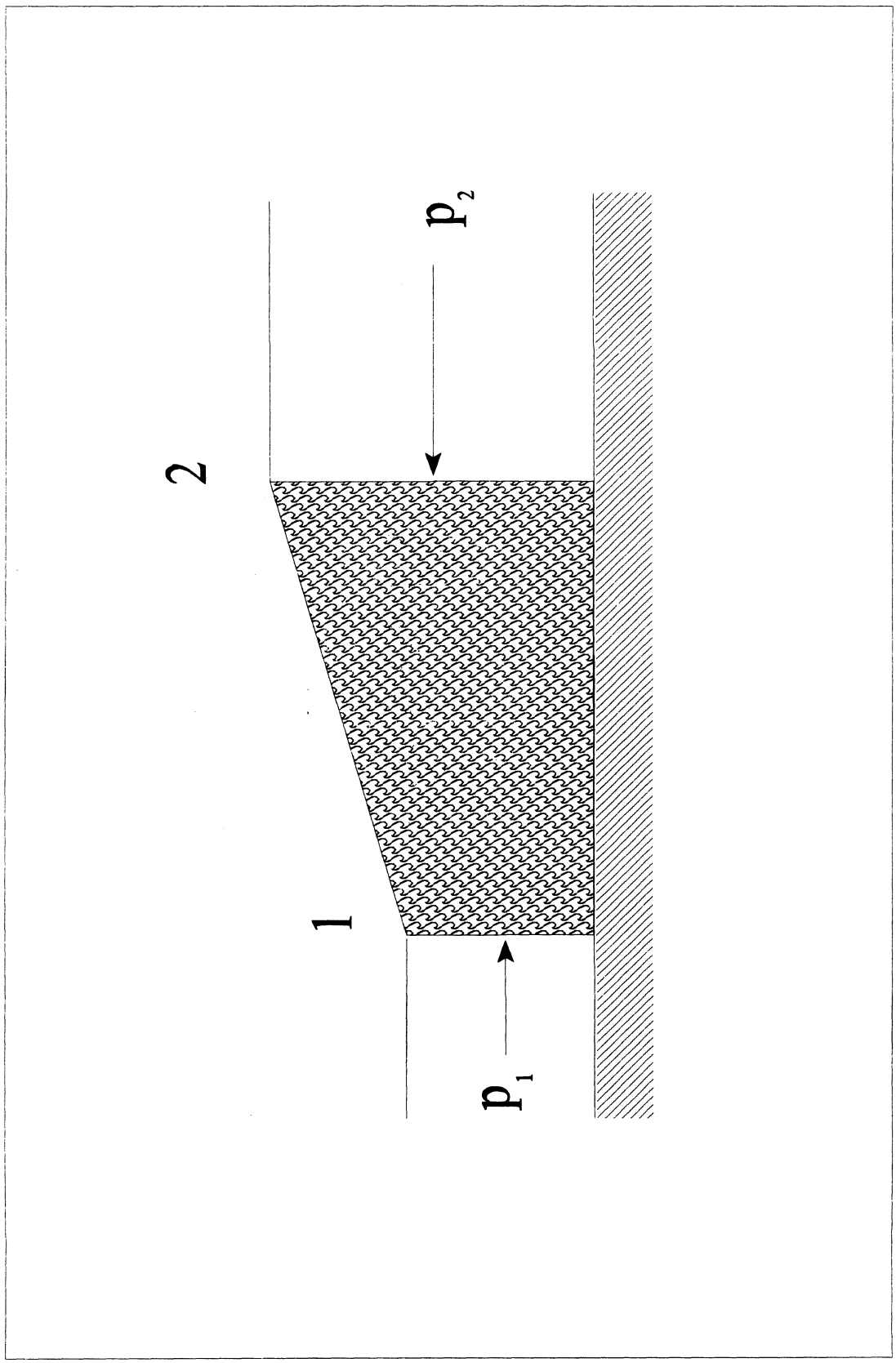

Figure 3- 4: The forces acting on the jump

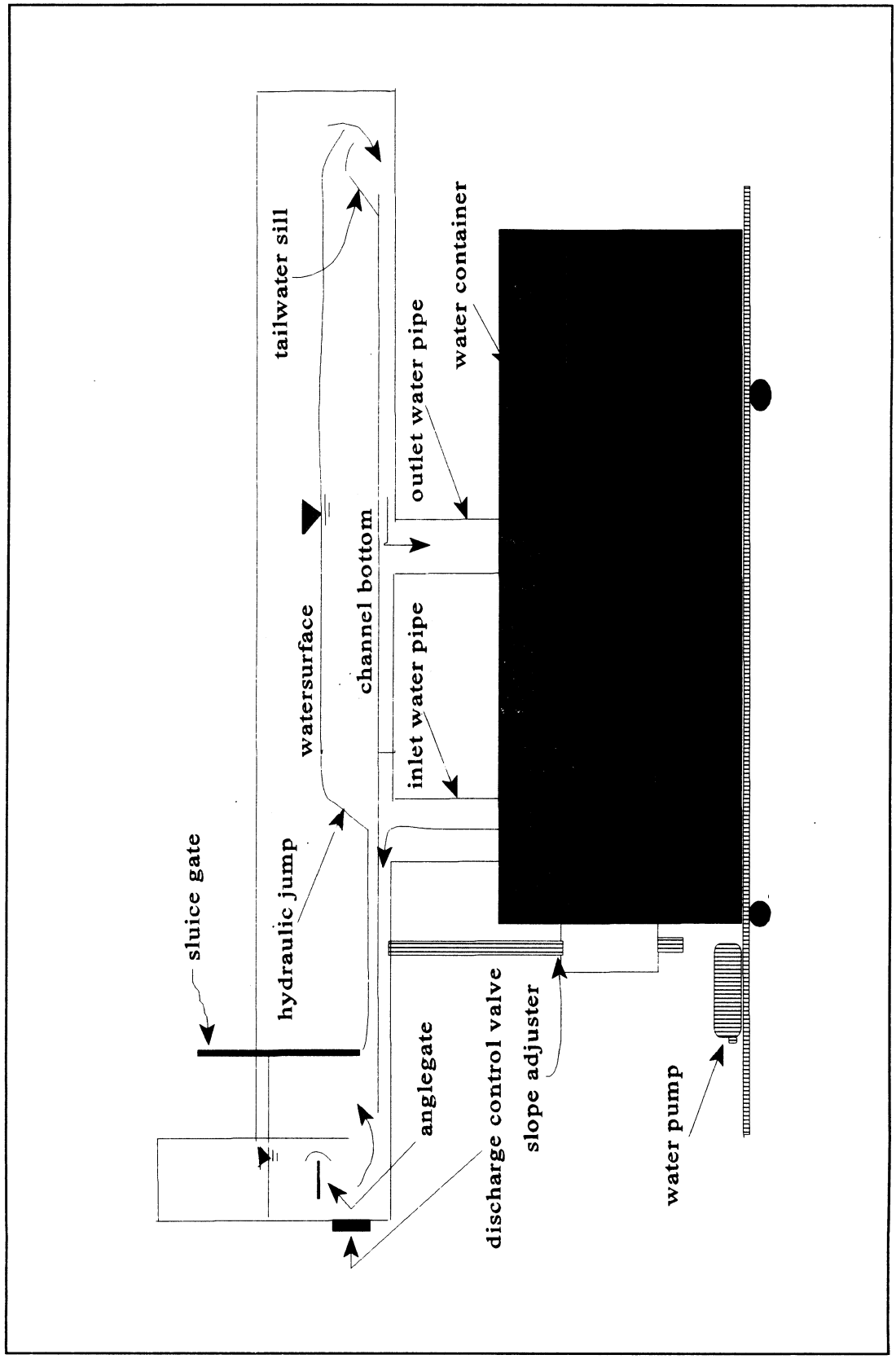

Figure 3-5: the model of the channel

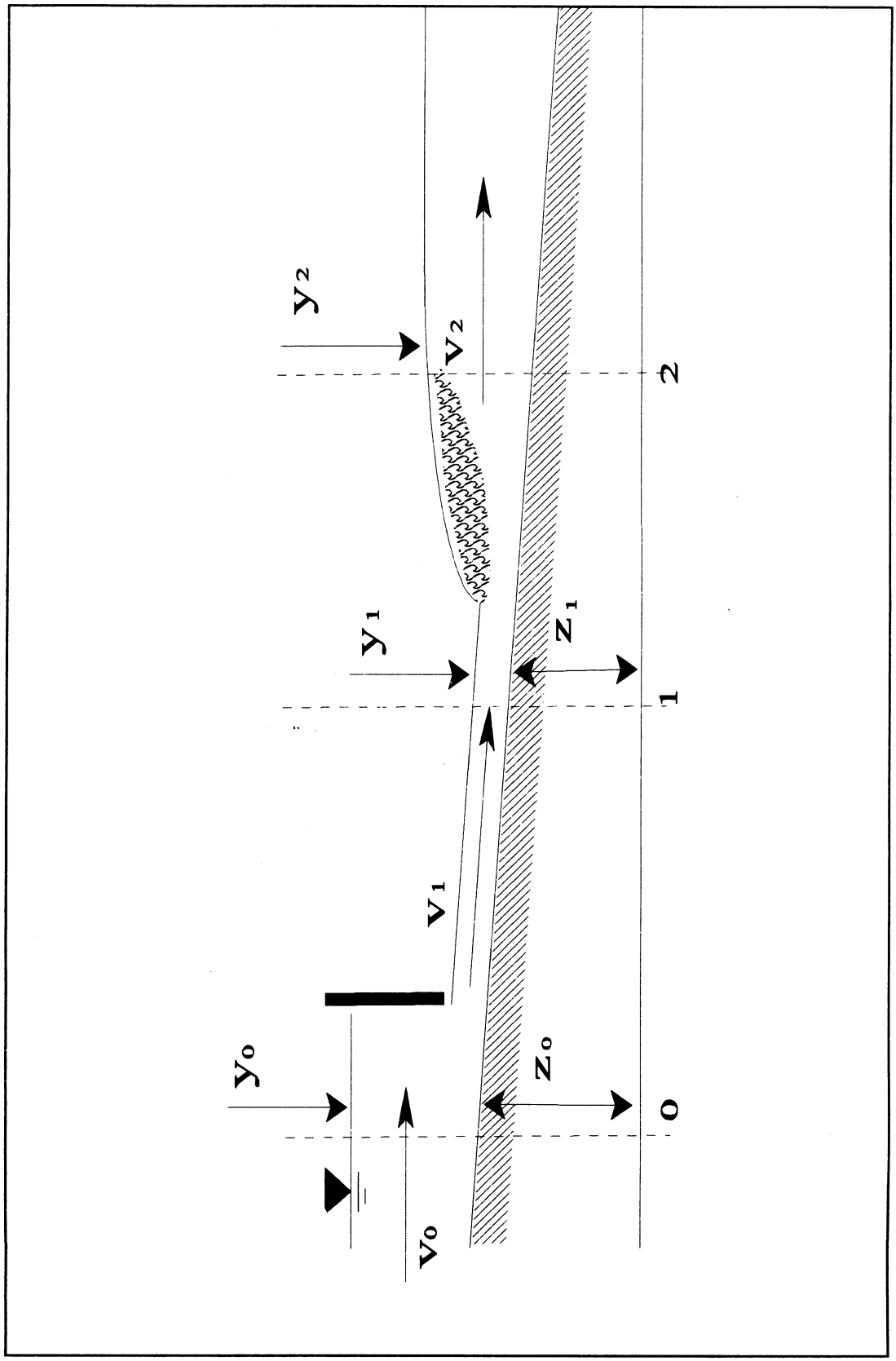

Figure 3-6: The channel section profiles

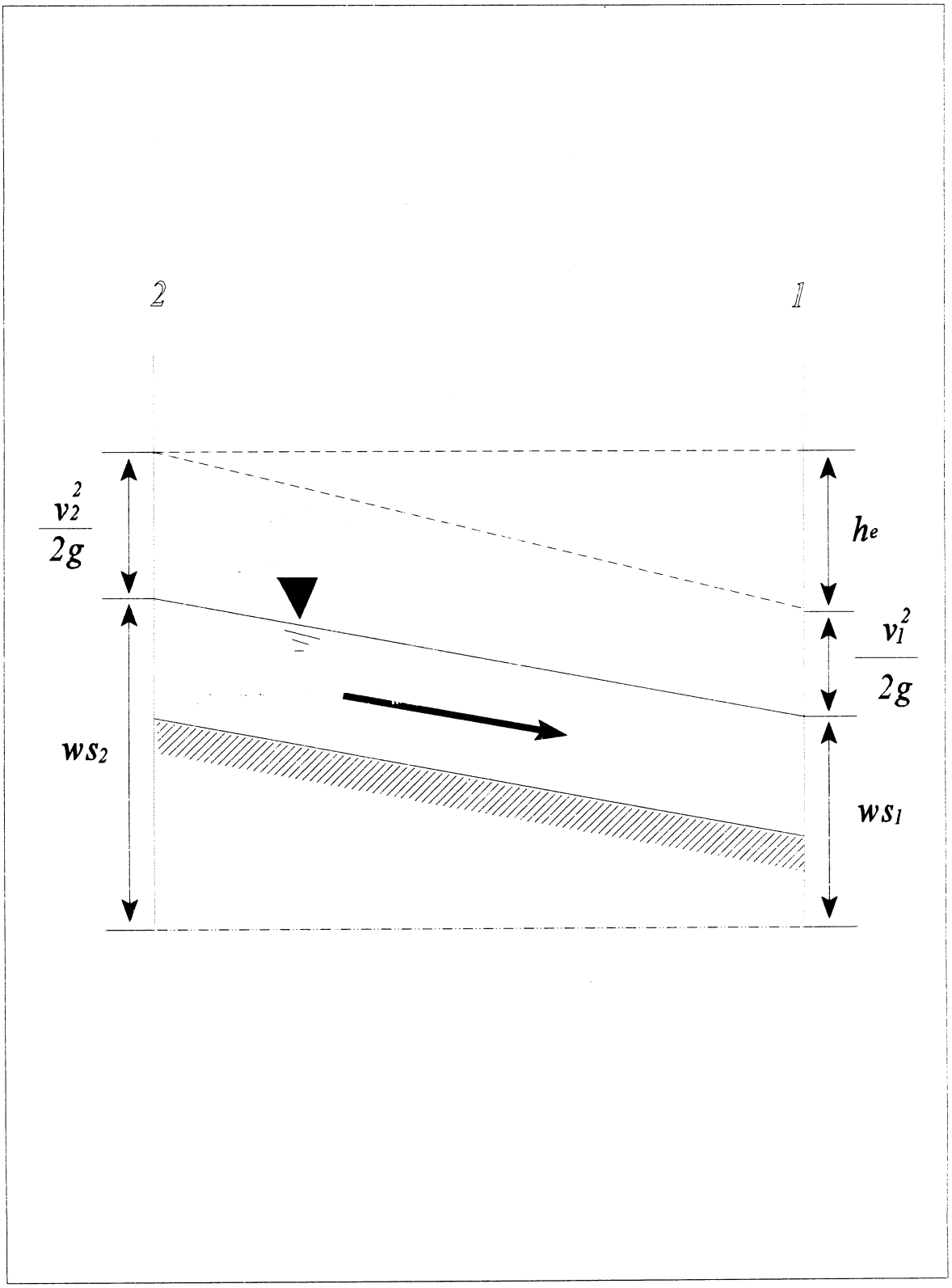

Figure 3-7: The energy profile of the water flow

CHAPTER IV. RESULTS AND DISCUSSION

The distance between the beginning and the end of a hydraulic jump is defined as the jump length, which usually moves up and down in the channel and is difficult to measure. Basically, the section of water surface starting to rise and having rollers coming out was regarded as the beginning of the jump, and the section of the water surface having the most bubbles coming out from the water surface was considered the end of the jump. If we measure the distances from the beginnings to the ends of the jumps, the average of these distances can be taken as an average of jump length. The initial depth and sequent depth of the jump are the depths of the beginning and the end of a hydraulic jump, respectively. Because of the oscillating waves of the water surface, average initial and sequent depths are used in this study. The results, arranged as several groups, show the relationships between hydraulic parameters and will be discussed in the following sections.

IV.1 EXPERIMENTAL RESULTS FOR JUMP LENGTH

As described in Section III.3, experiments were conducted for channel bed slopes of θ = 1° to 5°. Measurements from the experiments and their related estimation are listed in Tables 4-1 to 4-5. In order to widen practical applications in engineering problems, a set of hydraulic dimensionless terms was arranged including Froude number, F_1, and ratio of the jump length and sequent depth, L_j/y_2, where L_j is the jump length and y_2 is the sequent depth. Table 4-1

gives the values of F_1 and L_j/y_2 for $\theta = 1°$ while Tables 4-2 to 4-5 list values of F_1 and L_j/y_2 for $\theta = 2°$ to 5°. The relationships between these two terms can be more clearly expressed by plotting L_j/y_2 vs. F_1. In general L_j/y_2 increases as F_1 increases. Figure 4-1 gives a best-fit curve of L_j/y_2 vs. F_1 for channel bed slope of $\theta = 1°$ while Figures 4-2 to 4-5 are curves for $\theta = 2°$ to 5^0. It shows that L_j/y_2 increases when F_1 increases and approaches to a constant when F_1 approaches a value 7 to 8. It also shows that with the same Froude number, L_j/y_2 is larger for a larger θ. As previously described, the length of the jump is the major factor in designing hydraulic structures for spillways. The experimental results of L_j/y_2 vs. F_1 provided a convenient means to determine hydraulic jump lengths for dividing a channel reach in the HEC-2 flow routing. These results provide a potential to locate the hydraulic jump by a computer simulation rather than a costly model test. To design a stilling basin, the length of stilling basin can be better estimated by knowing $L_j = (L_j/y_2)\ (y_2)$ if the sequent depth after the jump is determined.

The experiments in this study were conducted with a range of Froude number, 2.65 to 7.97, for varied channel bed slopes, 1° to 5°. As shown in Figure 4-6, the curves are very similar for channel bed slopes of 1° and 2°, but when the channel slopes greater than 2°, the curves significantly change. When the channel bed slopes are greater than 3°, curves of L_j/y_2 vs. F_1 become flatter than those with bed slopes of 1° and 2°. Theoretically, the forces acting on the water body within the jump include hydrostatic forces at both ends of the jump, the friction force caused by the channel bottom and wall, viscous force of water, and the gravity force if the channel is not horizontal. Results from this study show a significant effect of the

channel bed slope on the length of a hydraulic jump as given in Figure 4-6.

IV.2 GRAVITY AND FRICTION EFFECTS ON HYDRAULIC JUMP

Comparing the estimated sequent depth, y_{2tp}, from Equation 3-13 with that estimated from the model test, y_{2ep}, the y_{2tp} is always greater than y_{2ep} when the channel bed slope is less than or equal to 2° as shown in Tables 4-6 to 4-7. When the channel bed slope becomes larger than 4° and the initial Froude number is greater than 5.11, y_{2ep} become larger than y_{2tp} as also shown in Tables 4-9 and 4-10. Figures 4-8 to 4-12 are plots for comparison of y_{2tp} and y_{2ep} at varied channel bed slopes. This interesting phenomenon can be explained in the following.

Figure 4-7 shows the control volume of a hydraulic jump occuring on an inclined channel. Applying the momentum equation to the control volume, the sum of total external forces, $\sum F$, should be equal to the change of the momentum per unit time, ΔM. To simplify the analysis, the linear momentum in the channel bed direction is considered. This results in

$$\Sigma F_x = \Delta M \quad , \tag{4-1}$$

where:

ΣF_x = the sum of external forces involved in the hydraulic jump

along channel direction,
ΔM = the change rate of the momentum involved.

When the friction force is neglected, the following equation exists.

$$\Sigma F_x = W \sin \theta + P_1 - P_2 \quad , \tag{4-2}$$

where:

$W \sin \theta$ = the component of water weight in channel direction,
θ = the channel slope,
P_1 = the hydrostatic force at upstream end,
P_2 = the hydrostatic force at downstream end,

and

$$\Delta M = \frac{\gamma}{g} q (v_2 - v_1) \quad , \tag{4-3}$$

where:

γ = the water weight per unit volume,
g = the gravity acceleration,
q = the water discharge per unit width,
v_1 = the water mean velocity at upstream end,
v_2 = the water mean velocity at downstream end.

Since $P_1 = (1/2) (\gamma y_1^2) \cos \theta$ and $P_2 = (1/2) (\gamma y_2^2) \cos \theta$, Equation 4-1 can be rearranged into

$$W \sin\theta + \frac{1}{2}\gamma\left(y_1^2 - y_2^2\right)\cos\theta = \frac{\gamma}{g} q \left(v_2 - v_1\right) , \qquad (4\text{-}4)$$

where $v_2 = q / y_2$, and $v_1 = q / y_1$. Hence, Equation 4-4 can be rewritten as

$$\frac{W \tan\theta}{\gamma\left(y_1 - y_2\right)} + \frac{1}{2}\left(y_1 - y_2\right) = \frac{v_1^2 y_1^2}{g \cos\theta} \frac{1}{y_1 y_2} \qquad (4\text{-}5)$$

The expression of y_2 / y_1 can hence be in terms of F_1 as:

$$\frac{y_2}{y_1} = \frac{1}{2}\left(-1 + \sqrt{1 + 8 F_1^2 / \cos\theta - 4C}\right) , \qquad (4\text{-}6)$$

where:

$C = (y_2 / y_1^2)\{V_v \tan\theta / (y_1 - y_2)\}$
V_v = the water volume within the jump.

C is negative because $(y_1 - y_2) < 0$. For a given F_1 and y_1, y_2 can be computed by:

$$y_2 = \frac{1}{2} y_1 \left(-1 + \sqrt{1 + 8 F_1^2 / \cos\theta - 4C}\right) \qquad (4\text{-}7)$$

From Equation 4-7, the value of C decreases and the value of $8 F_1^2 / \cos\theta$ with an increase of the channel bed slope θ increases. This will result in the increase of y_2. As previously

described, the use of Equation 3- 13 to estimate the sequent depth for channel bed slopes 4° and 5° with large F_1 results in that y_{2ep} is greater than y_{2tp}. This can be explained by the increase of channel bed slope θ. The values of y_{2ep} were estimated from the model test that takes into account of the gravity component. Figures 4-11 and 4-12 shows these significant changes of y_{2tp} and y_{2ep}.

In Equation 4-4 the friction force was neglected. If the friction factor is considered, Equation 4-7 can be rewritten as

$$y_2 = \frac{1}{2} y_1 \left(-1 + \sqrt{1 + 8 F_1^2 / \cos\theta - 4 C'} \right) , \qquad (4\text{-}8)$$

where:

$$C' = (y_2 / y_1^2) \{ V_v \tan\theta / (y_1 - y_2) + [f_f / \gamma (y_1 - y_2)] \} \qquad (4\text{-}8a)$$

f_f = the friction force in the system.

When the channel slope is small, $8F_1^2/\cos\theta$ is close to $8F_1^2$ and $V_v \tan\theta$ in Equation 4-8a is close to 0; therefore, the last item $f_f / \gamma (y_1 - y_2)$ dominates in Equation 4-8a. This means that the sequent death is affected more by the friction than the gravity when the channel bed slope is small. Similarly, it can also be used to explain why the sequent depths y_{2tp} estimated by the Belanger equation were larger than y_{2ep} that is estimated by model test when the channel bed slope is small. There are no gravity and friction factors considered in the

Belanger equation, but in the model test they are included.

IV.3 L_j/y_1 VERSUS F_1

The relation of L_j/y_2 vs. F1 has been explained in section IV.1 and expressed by Figures 4-1 to 4-6. Since y_1 and y_2 are functions of each other, Equation 3-14 can be rewritten as

$$F = f\left(F_1, \frac{L_j}{y_1}\right) \tag{4-9}$$

Estimation of the the ratio L_j/y_1 and initial Froude numbers F_1 were presented in Tables 4-1 to 4-5. Figure 4-13 to 4-17 graphically illustrate the relation of L_j/y_1 vs. F_1 for channel bed slopes of 1° to 5° and show that there is a linear relation between L_j/y_1 and F_1. Furthermore, Figure 4-18 provides a comparsion for all cases that the linear relation between L_j/y_1 and F_1 has an about 35° with F_1-axis.

IV.4 JUMP HEIGHT AND FROUDE NUMBER

The jump height, is defined as the difference of water depths before and after a hydraulic jump, (y_2 - y_1). Graphical plots of (y_2 - y_1) vs. F_1 show that there are smooth

curves existing between the jump height and Froude number, F_1, for varied channel bed slopes, 1° to 5°, respectively, as Given in Figures 4-19 to 4-23. Figure 4-24 provides plots of comparison for Figure 4-19 to 4-23 and shows that the jump height increases as θ increases for a given F_1. This relation provides valuable information for a stilling basin design, such as determining the size of a stilling basin and the spillway channel height.

IV. 5 RATIO OF WATER DEPTHS AND FROUDE NUMBER

To further explore the relationship between water depths of a hydraulic jump and Froude number, plots of y_2/y_1 vs. F_1 are presented in Figure 4-25 to 4-29. These figures show that the trend of the relationship between y_2/y_1 and F_1 is a linear line and its slope increases with the channel bed slope, θ, as given in Figure 4-30. This information is valuable for designing a hydraulic structure of a stilling basin. When designing a stilling basin, if channel upstream conditions, y_1 and F_1, are confined, an estimation of tailwater from these prepared plots can be used to ensure the jump to be formed in the stilling basin. Given a spillway channel and adjustable conditions , i.e., y_1 and F_1, the sequent depth y_2 can be estimated from these developed plots. To establish the sequent depth y_2 within the stilling basin, one can adjust the height of the sill to control the tailwater depth. This will lead to a possibility of using the HEC-2 flow routing to determine the location of the sequent depth easily.

Table 4-1: Experimental measurements and related estimation for $\theta = 1^{\circ}$

Test No.	y_0	y_1	y_2	L_j	F_1	L_j/y_2	L_j/y_1	y_2-y_1	y_2/y_1
1	8.10	2.50	6.50	23.50	2.41	3.62	9.40	4.00	2.60
2	9.00	2.40	6.60	27.00	2.65	4.09	11.25	4.20	2.75
3	10.00	2.30	6.80	31.50	2.90	4.63	13.70	4.50	2.96
4	11.00	2.20	7.10	33.50	3.15	4.72	15.23	4.90	3.23
5	12.30	2.10	7.40	36.00	3.39	4.86	17.14	5.30	3.52
6	13.20	1.95	7.60	38.50	3.62	5.07	19.74	5.65	3.90
7	14.10	1.90	7.70	40.50	3.82	5.26	21.32	5.80	4.05
8	15.50	1.85	8.00	43.50	4.06	5.44	23.51	6.15	4.32
9	16.70	1.80	8.30	47.00	4.30	5.66	26.11	6.50	4.61
10	18.40	1.70	8.80	50.50	4.57	5.74	29.71	7.10	5.18
11	19.80	1.60	9.00	52.50	4.91	5.83	32.81	7.40	5.63
12	20.60	1.55	9.10	53.50	5.11	5.88	34.52	7.55	5.87
13	21.60	1.50	9.20	55.00	5.34	5.98	36.67	7.70	6.13
14	23.40	1.40	9.40	56.50	5.78	6.01	40.36	8.00	6.71
15	24.30	1.36	9.50	58.00	5.97	6.11	42.65	8.14	6.99
16	25.50	1.28	9.70	60.50	6.32	6.24	47.27	8.42	7.58
17	26.50	1.22	9.85	62.00	6.56	6.29	50.82	8.63	8.07
18	27.60	1.20	10.00	63.50	6.77	6.35	52.92	8.80	8.33
19	28.50	1.18	10.10	65.00	6.94	6.44	55.08	8.92	8.56
20	29.50	1.15	10.30	68.00	7.13	6.60	59.13	9.15	8.96

y_0 : The water depth of the model before the sluice gate
y_1 : The initial water depth of the model
y_2 : The sequent water depth of the model
L_j : The jump length of the model
F_1 : The initial Froude number
θ : Channel bed slope

Table 4-2: Experimental measurements and related estimation for $\theta = 2^{\circ}$

Test No.	y_0	y_1	y_2	L_j	F_1	L_j/y_2	L_j/y_1	y_2-y_1	y_2/y_1
1	8.00	2.50	6.70	26.50	2.47	3.96	10.60	4.20	2.68
2	9.00	2.40	7.10	30.00	2.74	4.23	12.50	4.70	2.96
3	10.50	2.20	7.60	34.00	3.15	4.47	15.45	5.40	3.45
4	11.10	2.10	7.80	37.00	3.23	4.74	17.62	5.70	3.71
5	12.20	2.00	8.00	40.00	3.53	5.00	20.00	6.00	4.00
6	13.30	1.95	8.20	44.00	3.76	5.37	22.56	6.25	4.21
7	14.50	1.85	8.50	47.50	4.01	5.59	25.68	6.65	4.59
8	15.60	1.75	8.80	50.00	4.27	5.68	28.57	7.05	5.03
9	17.00	1.67	9.00	51.50	4.60	5.72	30.84	7.33	5.39
10	18.10	1.60	9.20	53.50	4.87	5.82	33.44	7.60	5.75
11	19.30	1.52	9.40	55.50	5.11	5.90	36.51	7.88	6.18
12	20.70	1.48	9.60	57.50	5.38	5.99	38.85	8.12	6.49
13	21.80	1.42	9.80	59.00	5.66	6.02	41.55	8.38	6.90
14	22.90	1.35	10.00	61.00	5.87	6.10	45.19	8.65	7.41
15	23.80	1.30	10.15	62.50	6.12	6.16	48.08	8.85	7.81
16	24.80	1.26	10.30	64.00	6.36	6.21	50.79	9.04	8.17
17	26.10	1.21	10.45	66.00	6.68	6.32	54.55	9.24	8.64
18	27.00	1.18	10.60	68.00	6.81	6.42	57.63	9.42	8.98
19	28.90	1.10	10.80	69.50	7.33	6.44	63.18	9.70	9.82

y_0 : The water dephh of the model before the sluice gate
y_1 : The initial water depth of the model
y_2 : The sequent water depth of the model
L_j : The jump length of the model
F_1 : The initial Froude number
θ : Channel bed slope

Table 4-3: Experimental measurements and related estimation for $\theta = 3°$

Test No.	y_0	y_1	y_2	L_j	F_1	L_j / y_2	L_j/y_1	y_2-y_1	y_2/y_1
1	8.10	2.40	7.00	29.00	2.78	4.14	12.08	4.60	2.92
2	9.10	2.28	7.50	32.50	3.04	4.33	14.25	5.22	3.29
3	10.00	2.16	8.00	37.50	3.30	4.69	17.36	5.84	3.70
4	11.00	2.04	8.40	41.00	3.49	4.88	20.10	6.36	4.12
5	12.20	1.90	8.60	43.00	3.73	5.00	22.63	6.70	4.53
6	13.40	1.85	8.90	45.50	3.99	5.11	24.59	7.05	4.81
7	14.30	1.80	9.10	47.50	4.10	5.22	26.39	7.30	5.06
8	15.50	1.75	9.30	50.50	4.36	5.43	28.86	7.55	5.31
9	16.50	1.68	9.50	52.00	4.62	5.47	30.95	7.82	5.65
10	17.60	1.60	9.70	53.50	4.91	5.52	33.44	8.10	6.06
11	19.20	1.50	10.00	56.00	5.22	5.60	37.33	8.50	6.67
12	20.60	1.45	10.20	57.00	5.51	5.59	39.31	8.75	7.03
13	22.10	1.35	10.40	59.00	5.90	5.67	43.70	9.05	7.70
14	23.70	1.30	10.70	61.00	6.23	5.70	46.92	9.40	8.23
15	25.10	1.20	10.95	63.00	6.71	5.75	52.50	9.75	9.13
16	27.10	1.15	11.10	66.00	7.09	5.95	57.39	9.95	9.65
17	28.40	1.10	11.30	68.00	7.43	6.02	61.82	10.20	10.27

y_0 : The water depth of the model before the sluice gate
y_1 : The initial water depth of the model
y_2 : The sequent water depth of the model
L_j : The jump length of the model
F_1 : The iniaial Froude number
θ : Channel bed slope

Table 4-4: Experimental measurements and related estimation for $\theta = 4^{\circ}$

Test No.	y_0	y_1	y_2	L_j	F_1	L_j / y_2	L_j/y_1	y_2-y_1	y_2/y_1
1	7.70	2.30	7.50	30.00	2.93	4.00	13.04	5.20	3.26
2	8.80	2.20	7.90	32.50	3.18	4.11	14.77	5.70	3.59
3	9.50	2.15	8.20	35.00	3.35	4.27	16.28	6.05	3.81
4	10.50	2.04	8.65	39.50	3.51	4.57	19.36	6.61	4.24
5	11.20	2.00	8.80	40.50	3.55	4.60	20.25	6.80	4.40
6	11.70	1.95	9.00	44.00	3.82	4.89	22.56	7.05	4.62
7	13.20	1.85	9.50	46.50	4.04	4.89	25.14	7.65	5.14
8	14.60	1.78	9.70	50.00	4.32	5.15	28.09	7.92	5.45
9	15.80	1.69	10.10	51.50	4.63	5.10	30.47	8.41	5.98
10	17.40	1.54	10.40	54.50	5.11	5.24	35.39	8.86	6.75
11	19.40	1.50	10.70	56.50	5.47	5.28	37.67	9.20	7.13
12	20.90	1.44	11.00	59.50	5.67	5.41	41.32	9.56	7.64
13	22.50	1.35	11.20	61.50	6.10	5.49	45.56	9.85	8.30
14	23.50	1.31	11.45	62.50	6.27	5.46	47.71	10.14	8.74
15	25.00	1.27	11.60	63.50	6.58	5.47	50.00	10.33	9.13
16	26.80	1.18	11.80	65.50	7.07	5.55	55.51	10.62	10.00
17	28.40	1.10	12.00	66.50	7.54	5.54	60.45	10.90	10.91

y_0 : The water depth of the model before the sluice gate
y_1 : The initial water depth of the model
y_2 : The sequent water depth of the model
L_j : The jump length of the model
F_1 : The initial Froude number
θ : Channel bed slope

Table 4-5: Experimental measurements and related estimation for $\theta = 5^{\circ}$

Test No.	y_0	y_1	y_2	L_j	F_1	L_j / y_2	l/y1	y_2-y_1	y_2/y_1
1	7.20	2.25	8.20	31.50	3.04	3.84	14.0	5.95	3.64
2	8.30	2.15	8.70	36.00	3.31	4.14	16.7	6.55	4.05
3	9.10	2.05	9.00	39.00	3.54	4.33	19.0	6.95	4.39
4	10.30	1.98	9.60	44.50	3.80	4.64	22.4	7.62	4.85
5	11.20	1.92	9.90	46.00	3.83	4.65	23.9	7.98	5.16
6	12.20	1.85	10.10	48.00	4.10	4.75	25.9	8.25	5.46
7	13.50	1.75	10.50	51.50	4.34	4.90	29.4	8.75	6.00
8	14.50	1.70	10.70	54.50	4.57	5.09	32.0	9.00	6.29
9	16.20	1.60	11.10	57.50	4.91	5.18	35.9	9.50	6.94
10	17.70	1.51	11.20	59.00	5.30	5.27	39.0	9.69	7.42
11	19.50	1.42	11.50	60.00	5.68	5.22	42.2	10.08	8.10
12	21.30	1.30	11.80	61.50	6.20	5.21	47.3	10.50	9.08
13	23.40	1.20	12.10	63.50	6.71	5.25	52.9	10.90	10.08
14	25.50	1.10	12.40	65.00	7.24	5.24	59.0	11.30	11.27
15	28.00	1.00	12.60	66.50	7.97	5.27	66.5	11.60	12.60

y_0 : The water depth of the model before the sluice gate
y_1 : The initial water depth of the model
y_2 : The sequent water depth of the model
L_j : The jump length of the model
F_1 : The initial Froude number
θ : Channel bed slope

Table 4-6: Comparison of sequent depths estimated by the Belanger equation and model test for channel bed slope = 1°

θ channel slope	F_1 initial Froude No.	y_{1p}(m) initial depth	y_{2tp}(m) sequent depths converted from the Belanger equation	y_{2ep}(m) sequent depths converted from experiment
1°	2.65	1.57	5.16	4.33
1°	3.62	1.28	5.95	4.99
1°	4.30	1.18	6.62	5.45
1°	5.78	0.92	7.07	6.17
1°	6.94	0.77	7.22	6.63

Table 4-7: Comparison of sequent depths estimated by the Belanger equation and model test for channel bed slope = 2°

θ channel slope	F_1 initial Froude No.	y_{1p}(m) initial depth	y_{2tp}(m) sequent depths converted from The Belanger equation	y_{2ep}(m) sequent depths converted from experiment
2°	2.74	1.57	5.36	4.66
2°	3.76	1.28	6.21	5.38
2°	4.87	1.05	6.73	6.04
2°	5.87	0.89	6.93	6.56
2°	6.81	0.77	7.08	6.96

Table 4-8: Comparison of sequent depths estimated by the Belanger equation and model test for channel bed slope = 3°

θ channel slope	F_1 initial Froude No.	y_{1p}(m) initial depth	y_{2tp}(m) sequent depths converted from The Belanger equation	y_{2ep}(m) sequent depths converted from experiment
3°	3.04	1.50	5.72	4.92
3°	4.10	1.18	6.29	5.97
3°	4.91	1.05	6.79	6.36
3°	6.23	0.85	7.11	7.02
3°	6.99	0.75	7.20	7.28

Table 4-9: Comparison of sequent depths estimated by the Belanger equation and model test for channel bed slope = 4°

θ channel slope	F_1 initial Froude No.	y_{1p}(m) initial depth	y_{2tp}(m) sequent depths converted from The Belanger equation	y_{2ep}(m) sequent depths converted from experiment
4°	3.18	1.44	5.82	5.18
4°	4.04	1.21	6.37	6.23
4°	5.11	1.01	6.82	6.82
4°	6.10	0.89	7.21	7.35
4°	7.07	0.77	7.36	7.74

Table 4-10: Comparison of sequent depths estimated by the Belanger equation and model test for channel bed slope = 5°

θ channel slope	F_1 initial Froude No.	y_{1p}(m) initial depth	y_{2tp}(m) sequent depths converted from The Belanger equation	y_{2ep}(m) sequent depths converted from experiment
5°	3.35	1.41	6.01	5.71
5°	4.34	1.15	6.50	6.89
5°	5.30	0.99	6.95	7.35
5°	6.20	0.85	7.07	7.74
5°	7.24	0.72	7.04	8.14

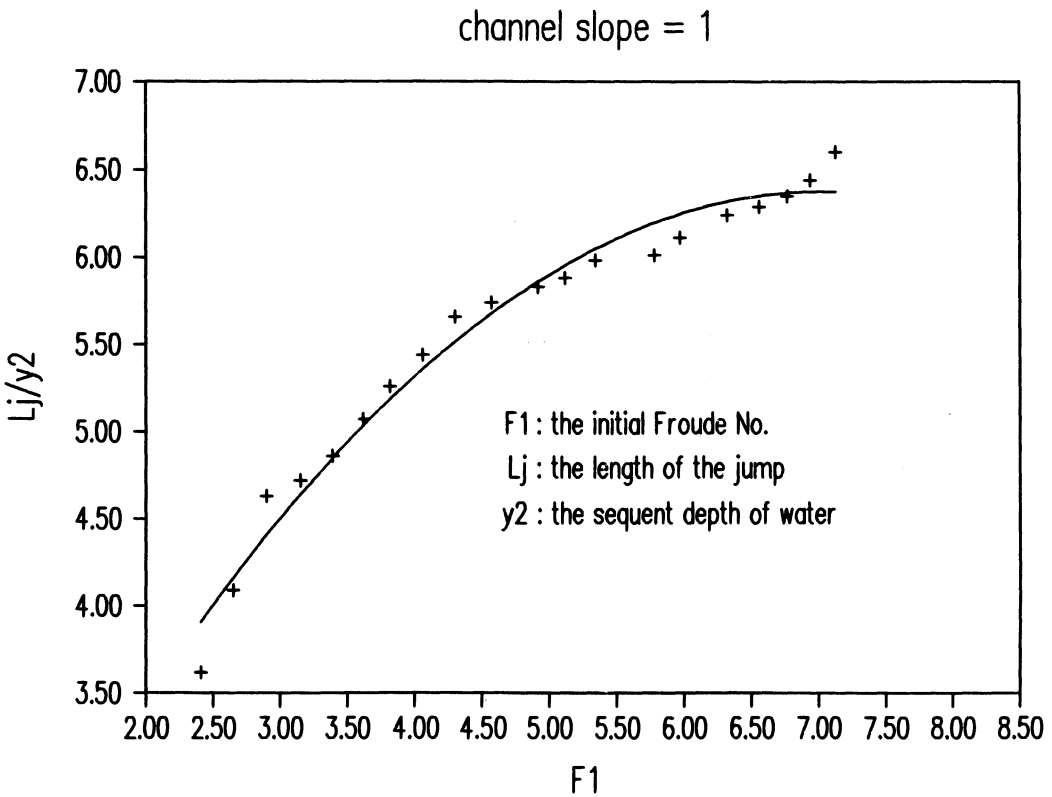

Figure 4-1 : Lj/y2 vs F1

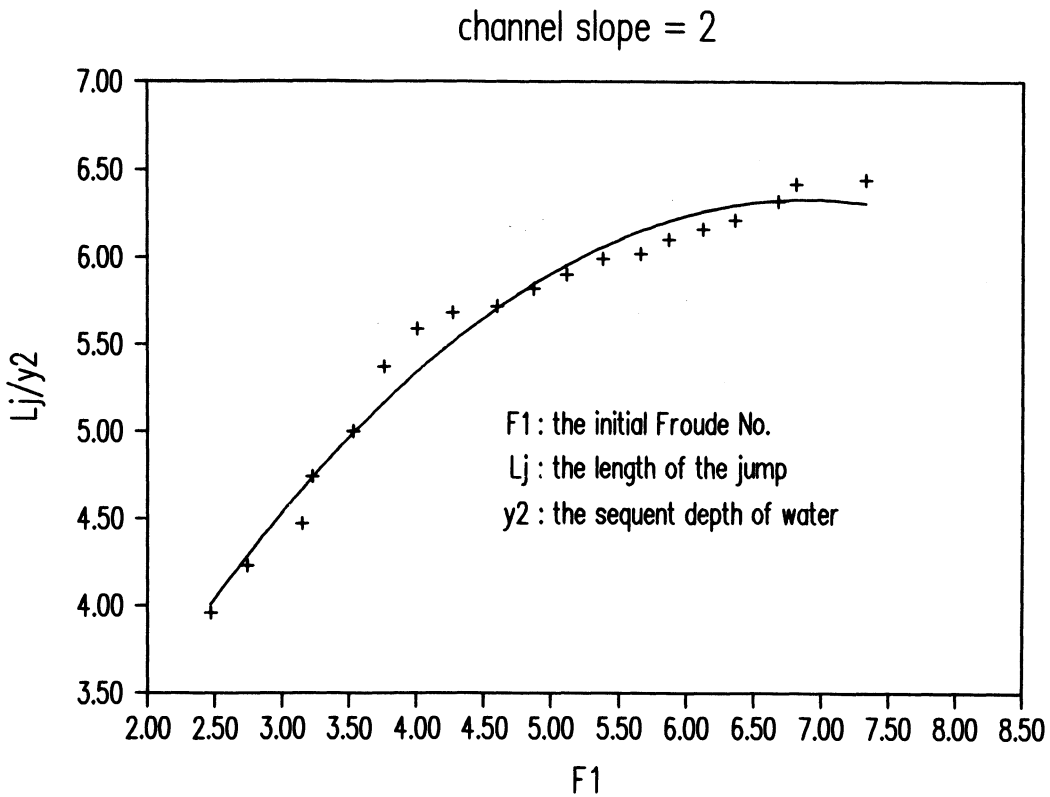

Figure 4-2 : Lj/y2 vs F1

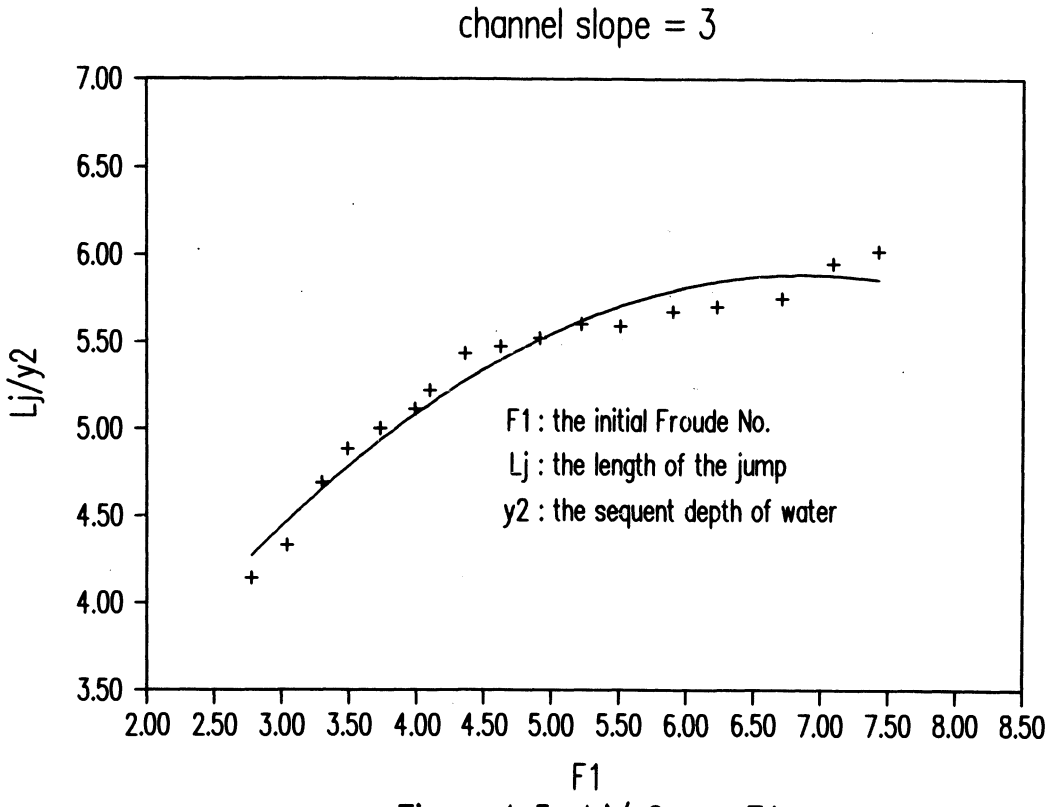

Figure 4-3 : Lj/y2 vs F1

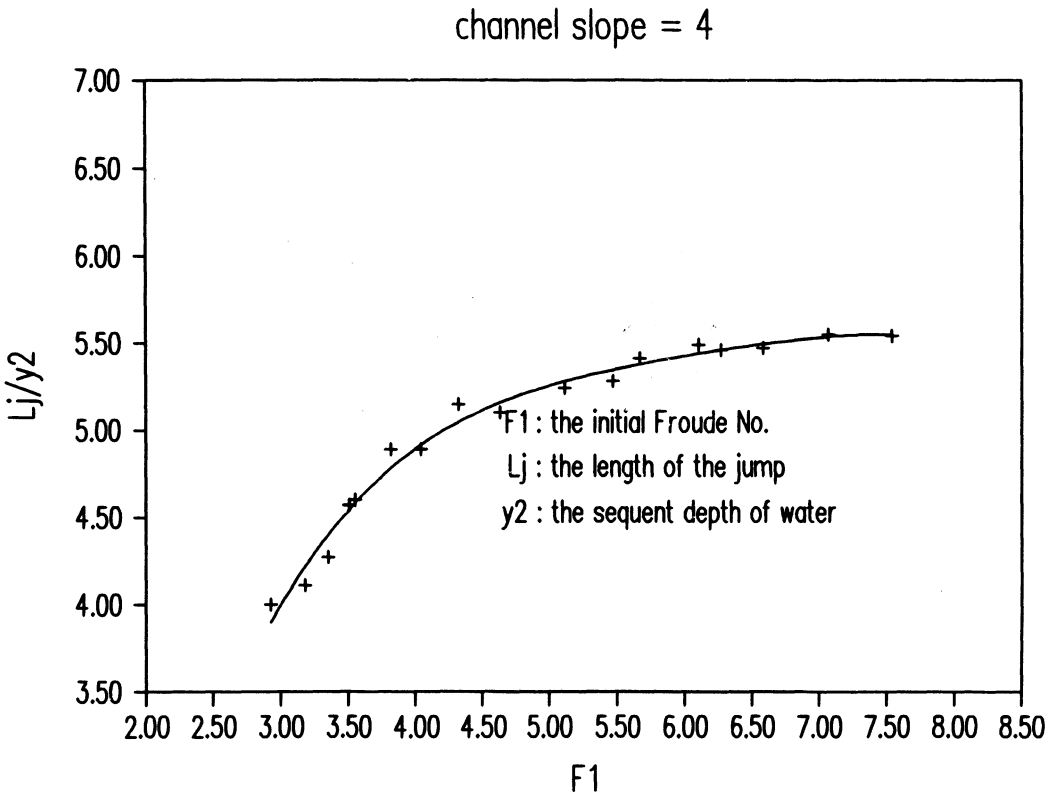

Figure 4-4 : Lj/y2 vs F1

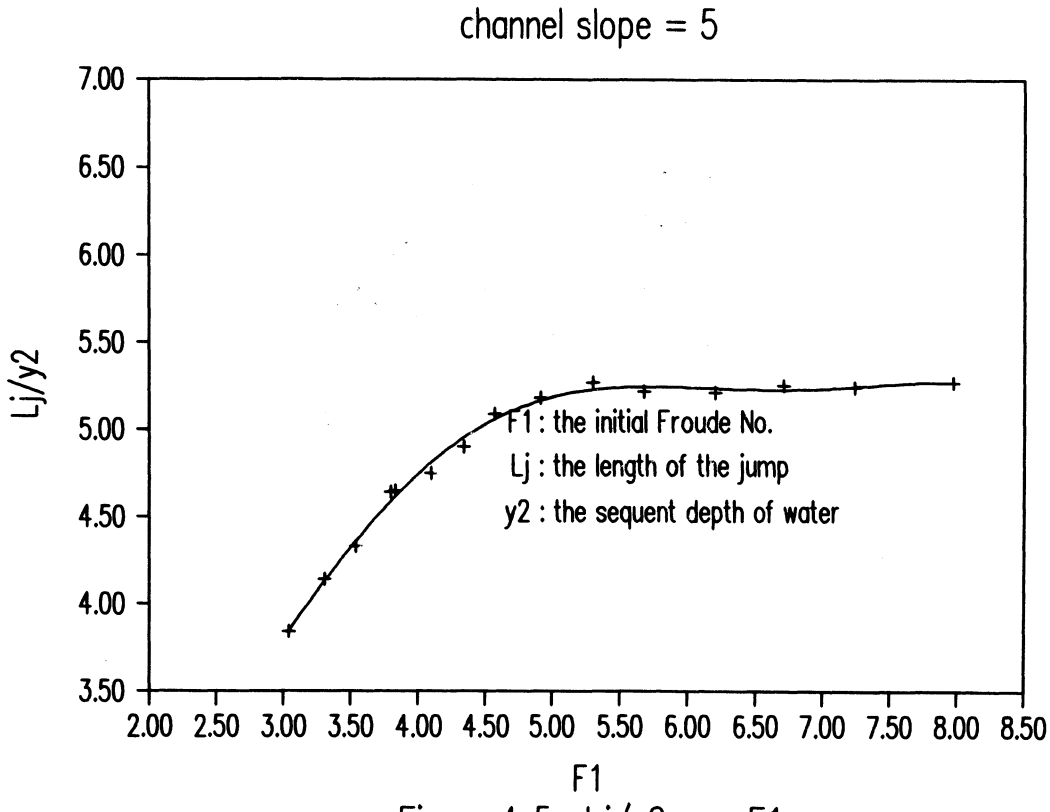

Figure 4-5 : Lj/y2 vs F1

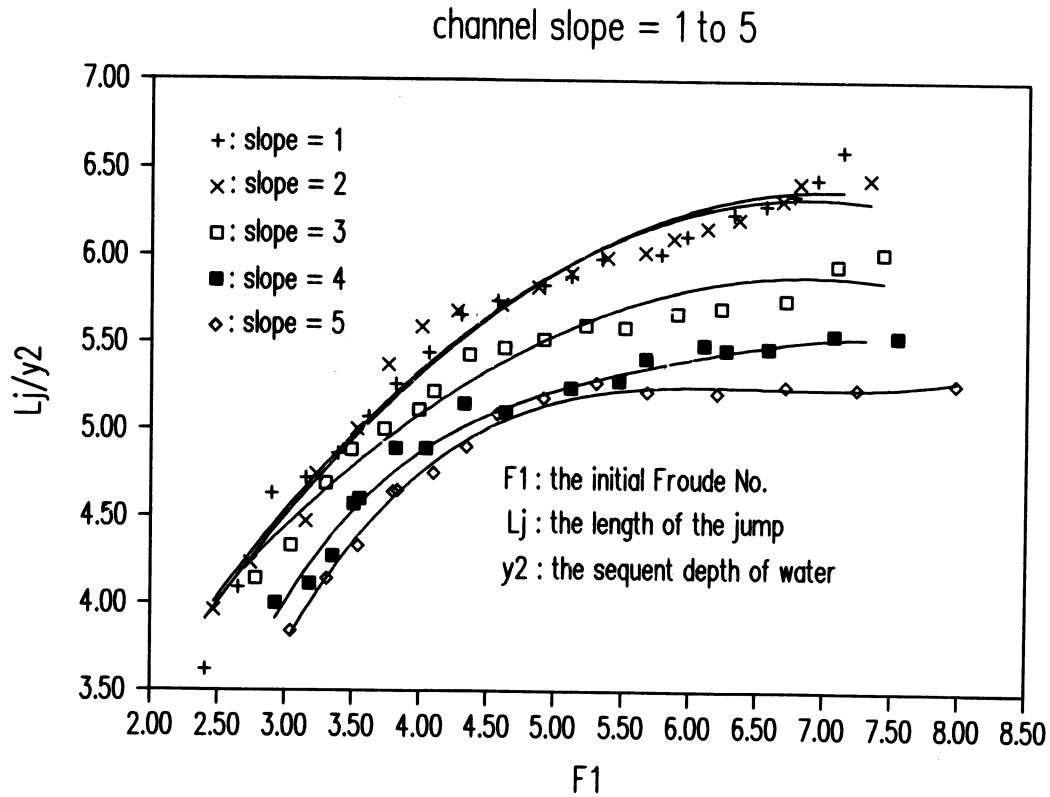

Figure 4-6 : Lj/y2 vs F1

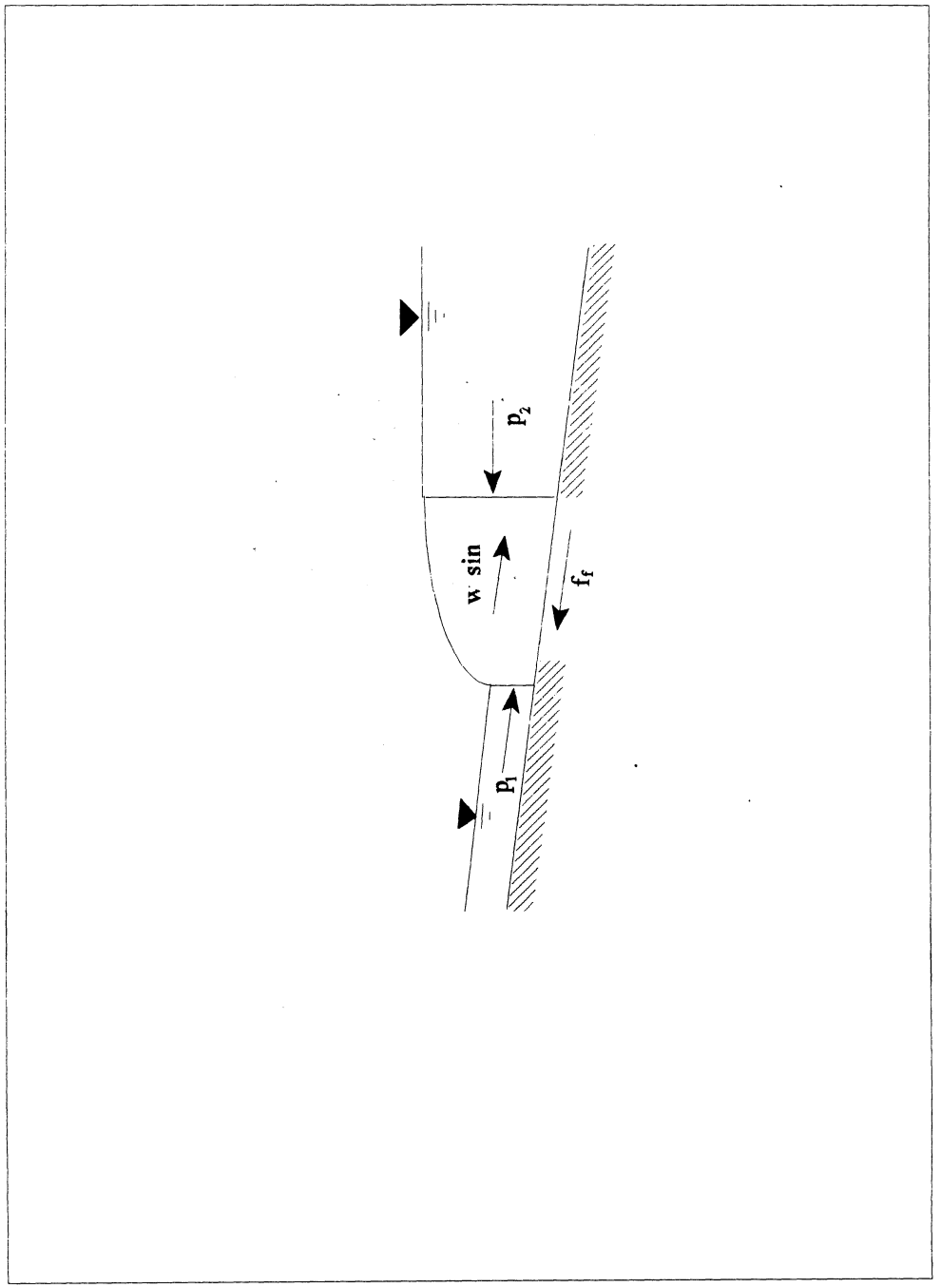

Figure 4-7: Forces involved in a hydraulic jump on an inclined channel

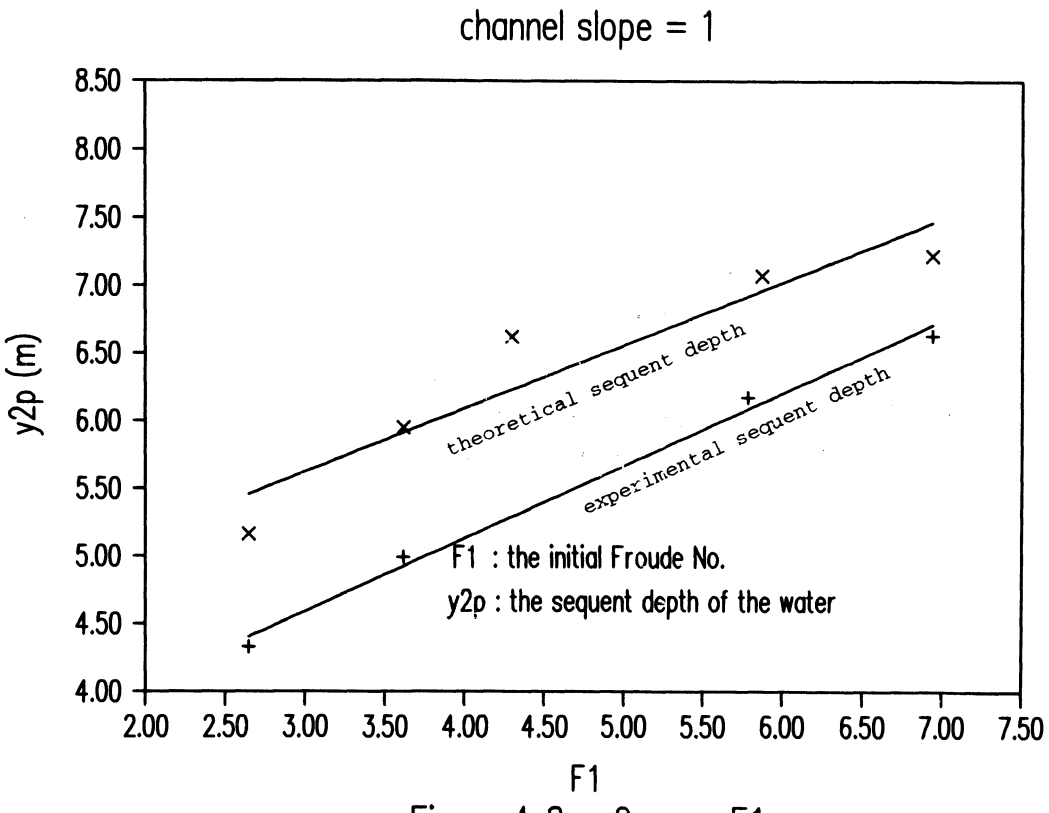

Figure 4-8 : y2p vs F1

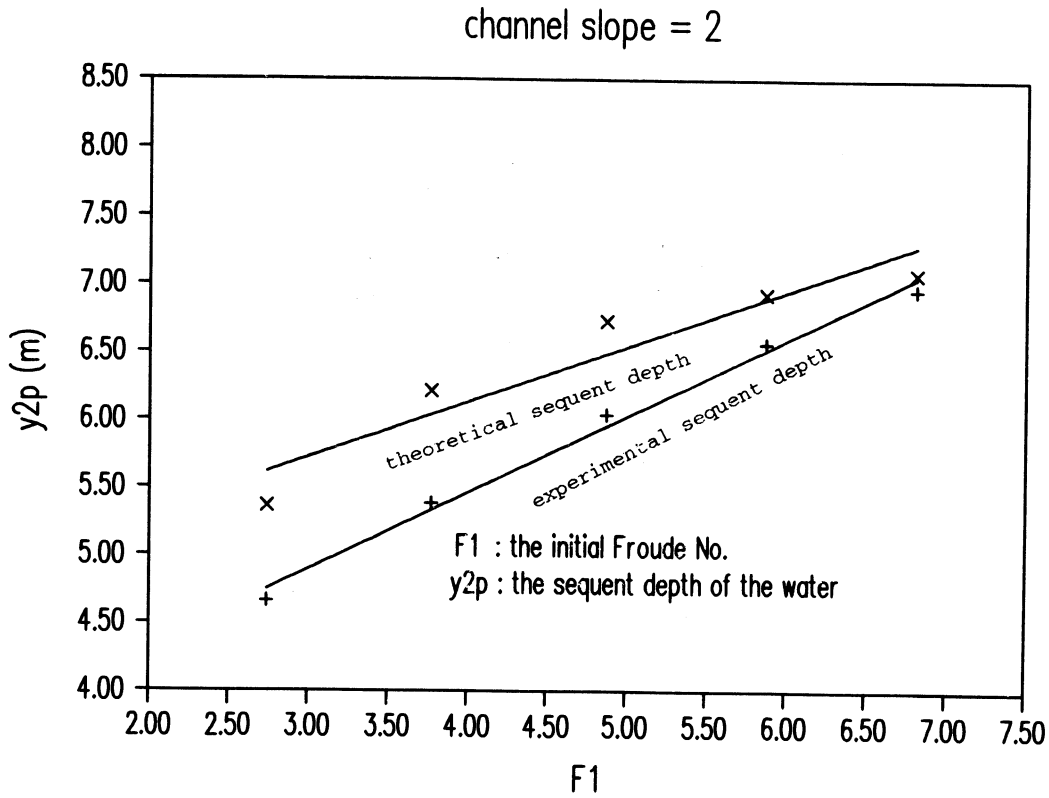

Figure 4-9 : y2p vs F1

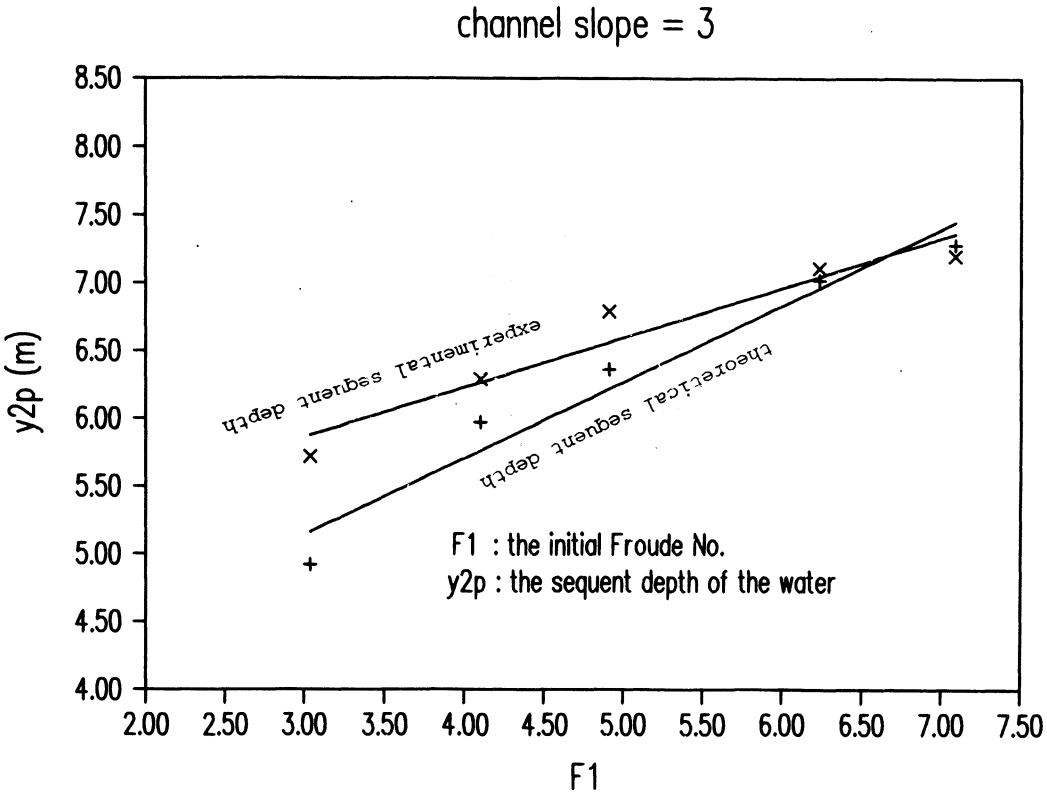

Figure 4-10 : y2p vs F1

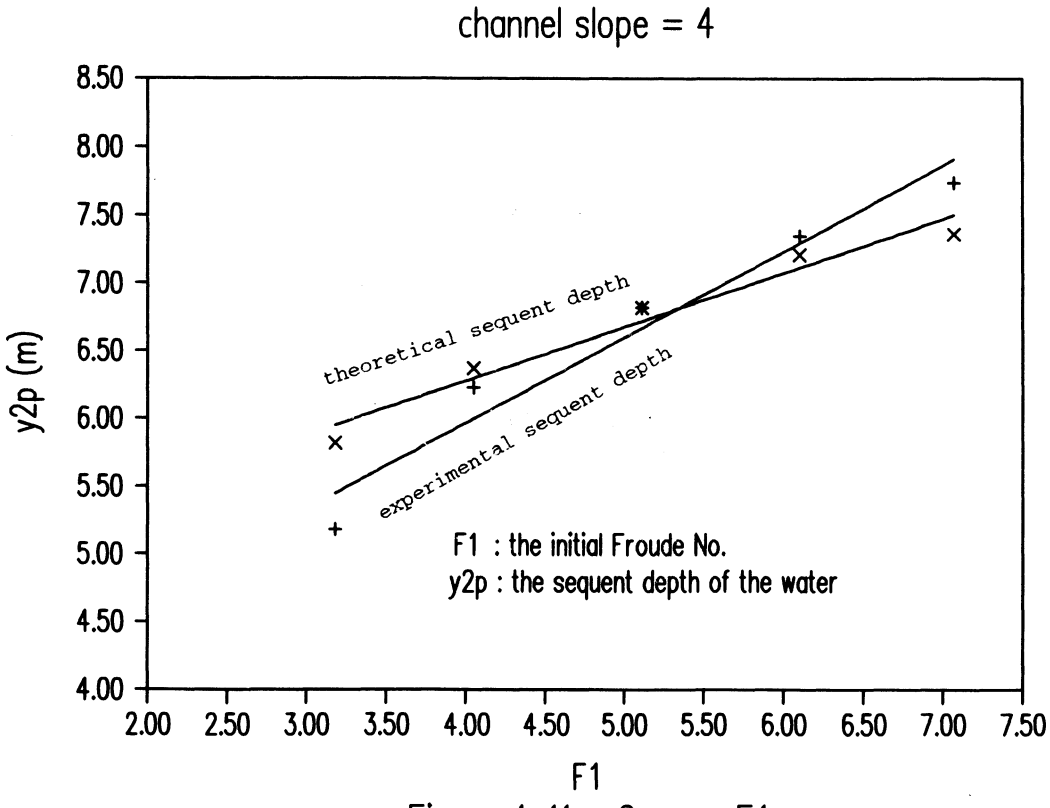

Figure 4-11 : y2p vs F1

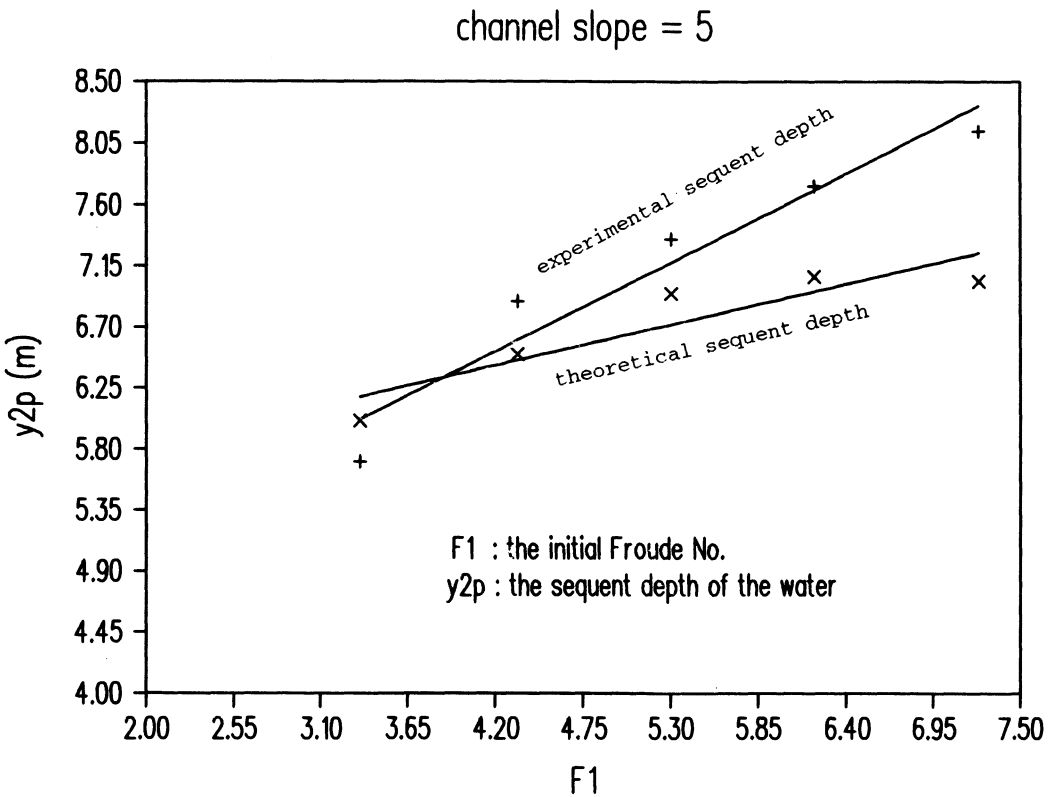

Figure 4-12 : y2p vs F1

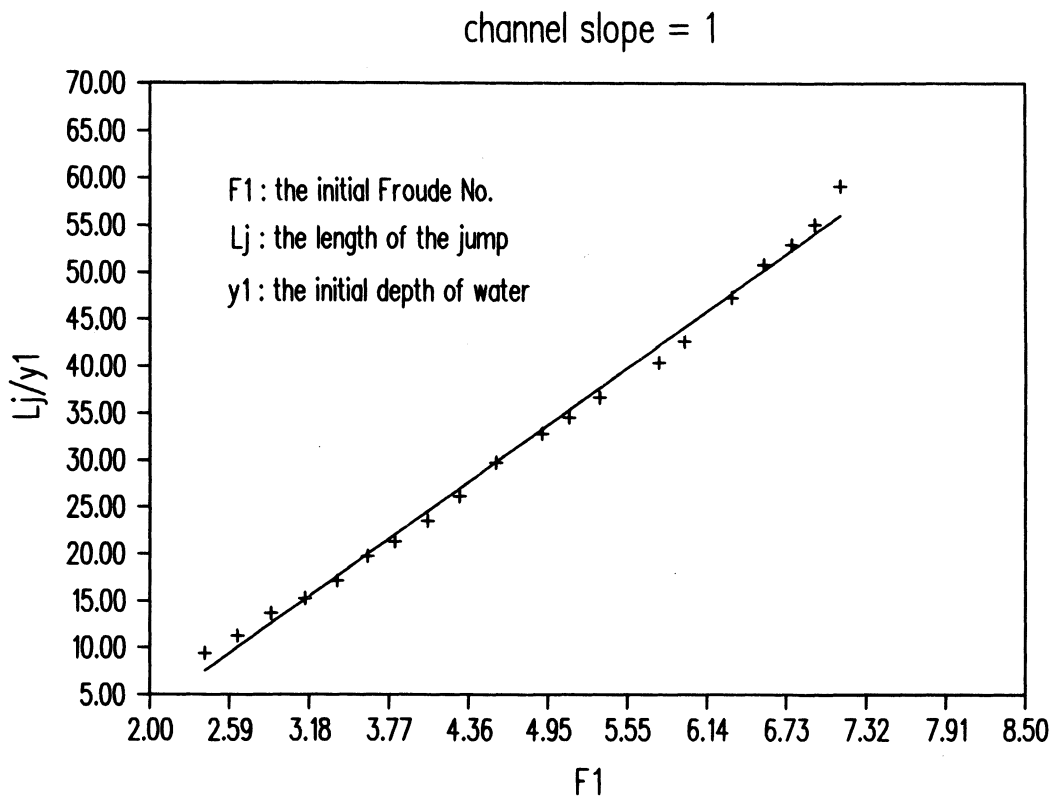

Figure 4-13 : Lj/y1 vs F1

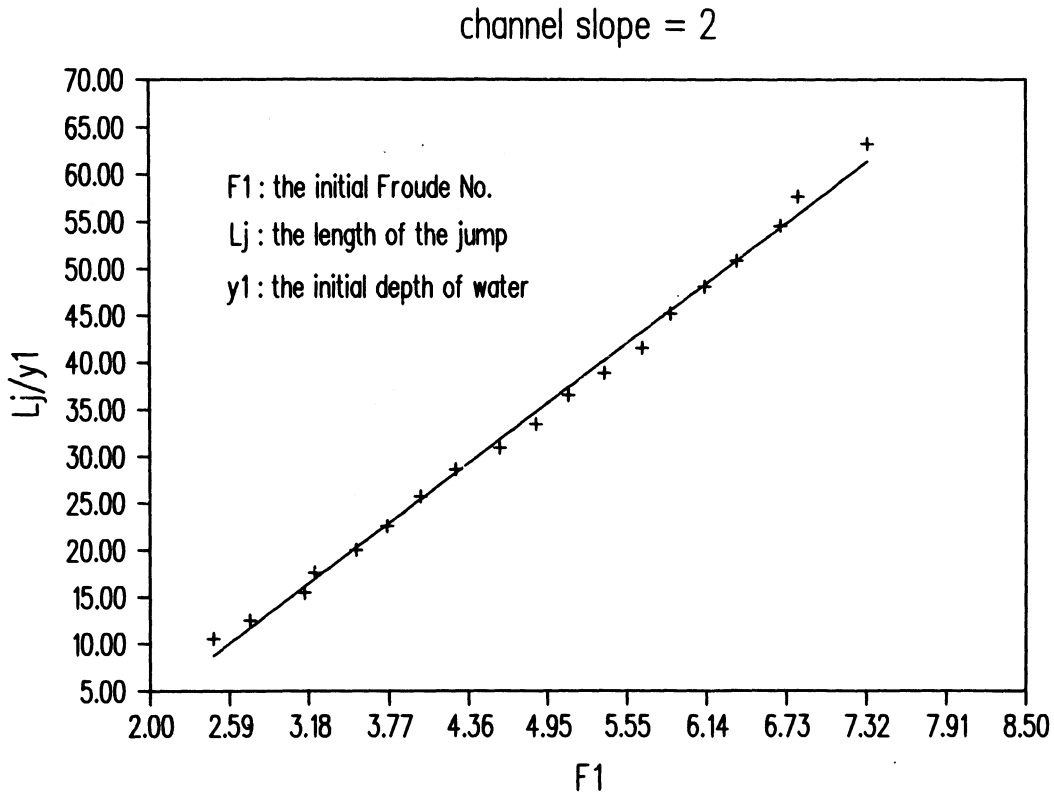

Figure 4-14 : Lj/y1 vs F1

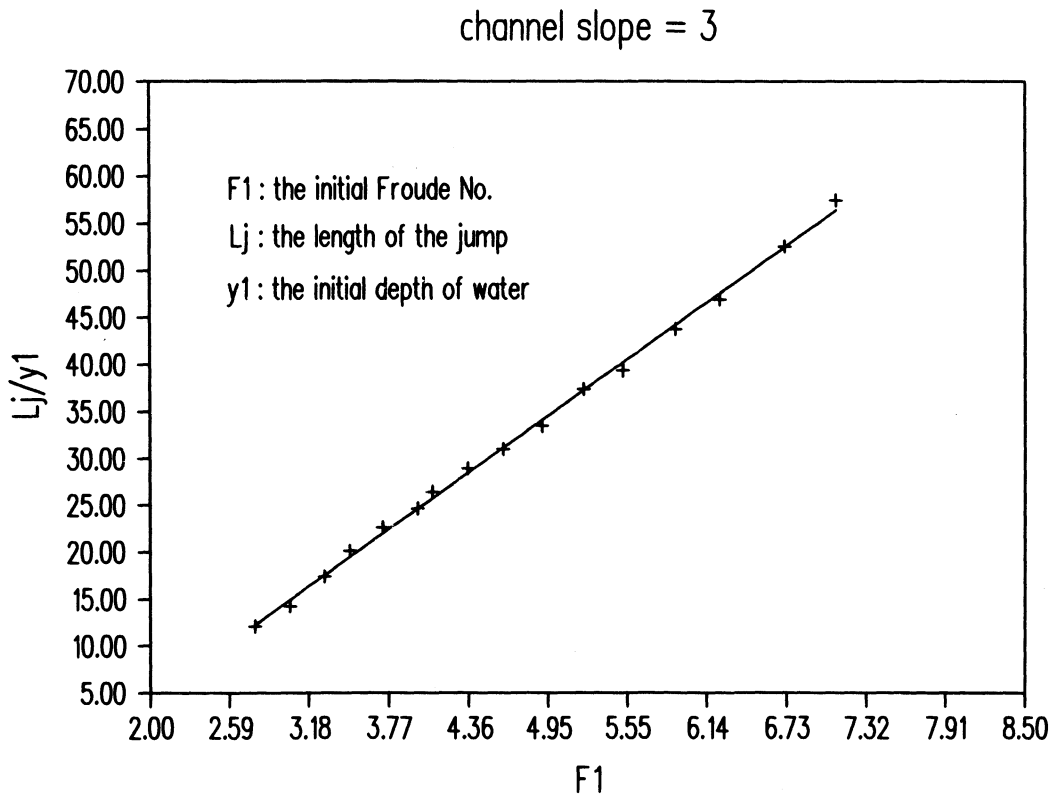

Figure 4-15 : Lj/y1 vs F1

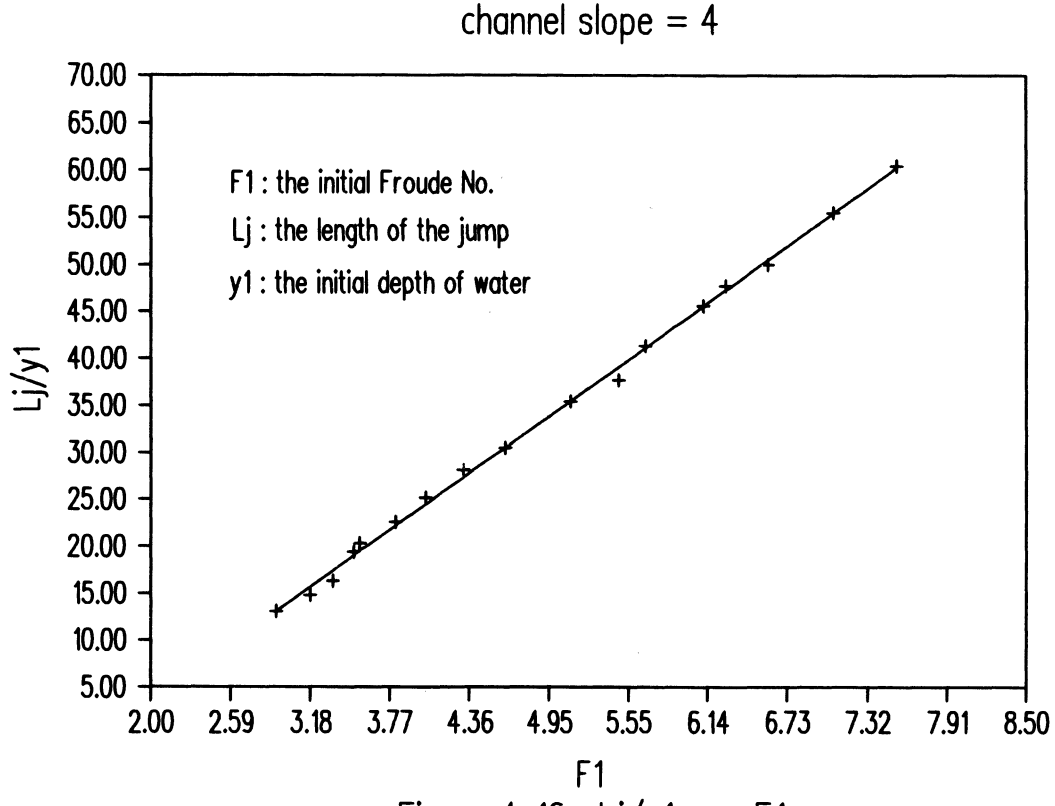

Figure 4-16 : Lj/y1 vs F1

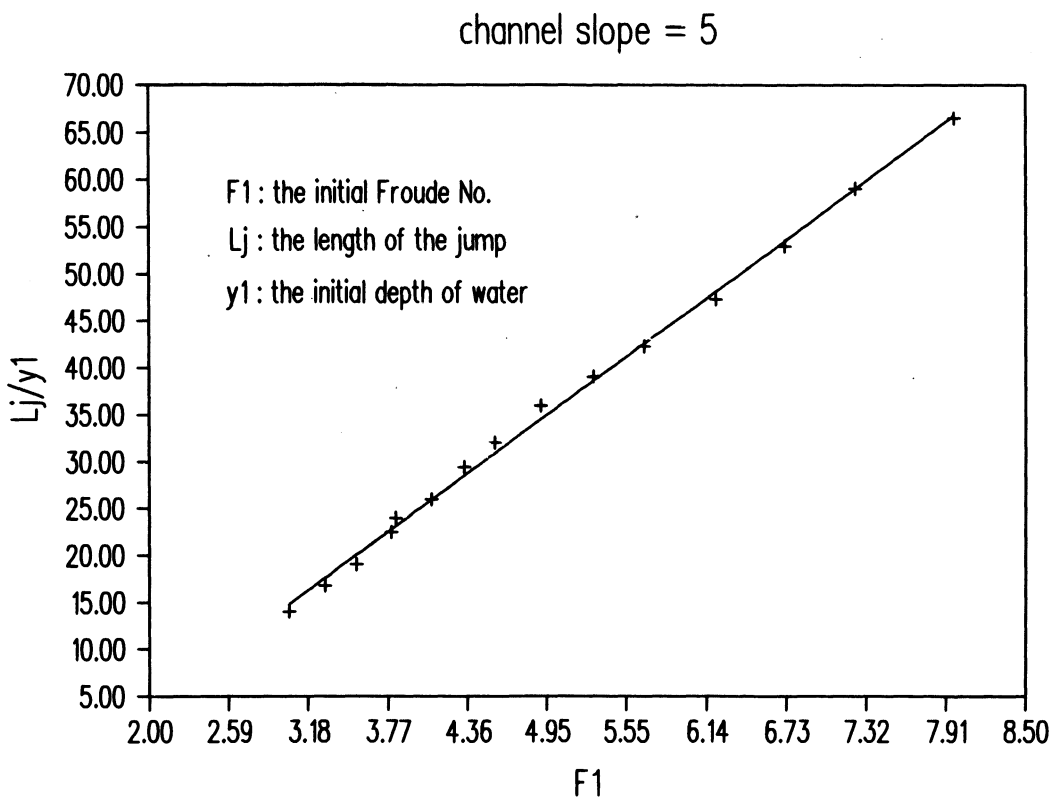

Figure 4-17 : Lj/y1 vs F1

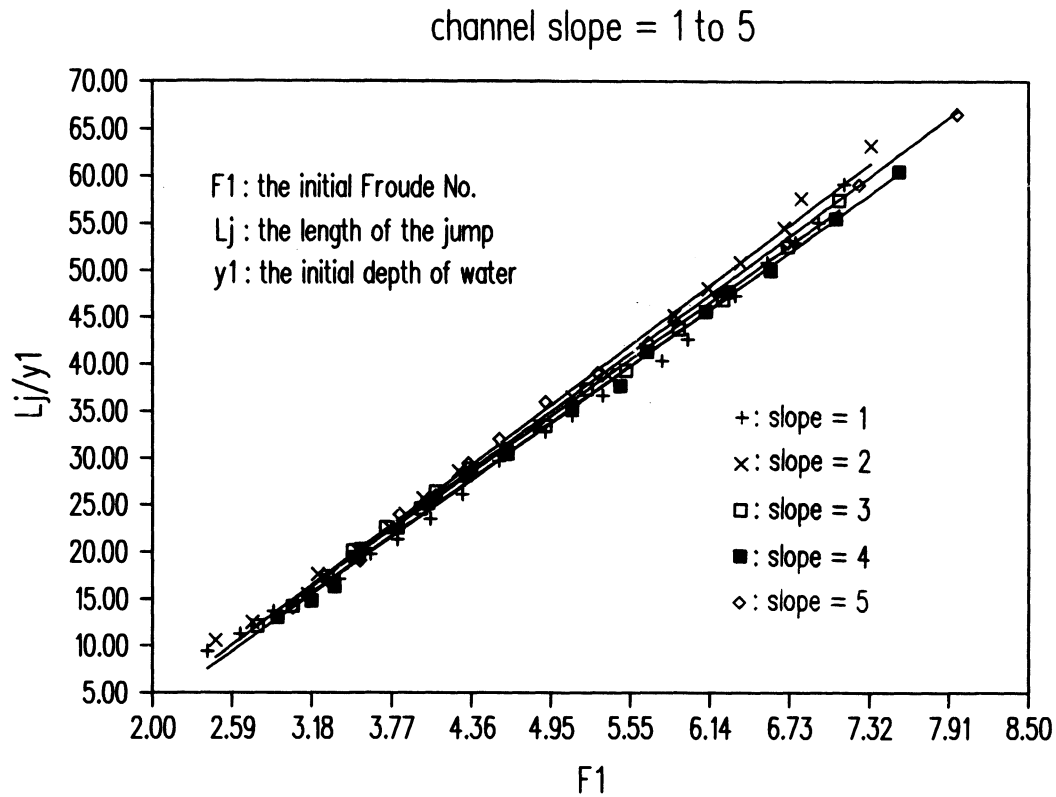

Figure 4-18 : Lj/y1 vs F1

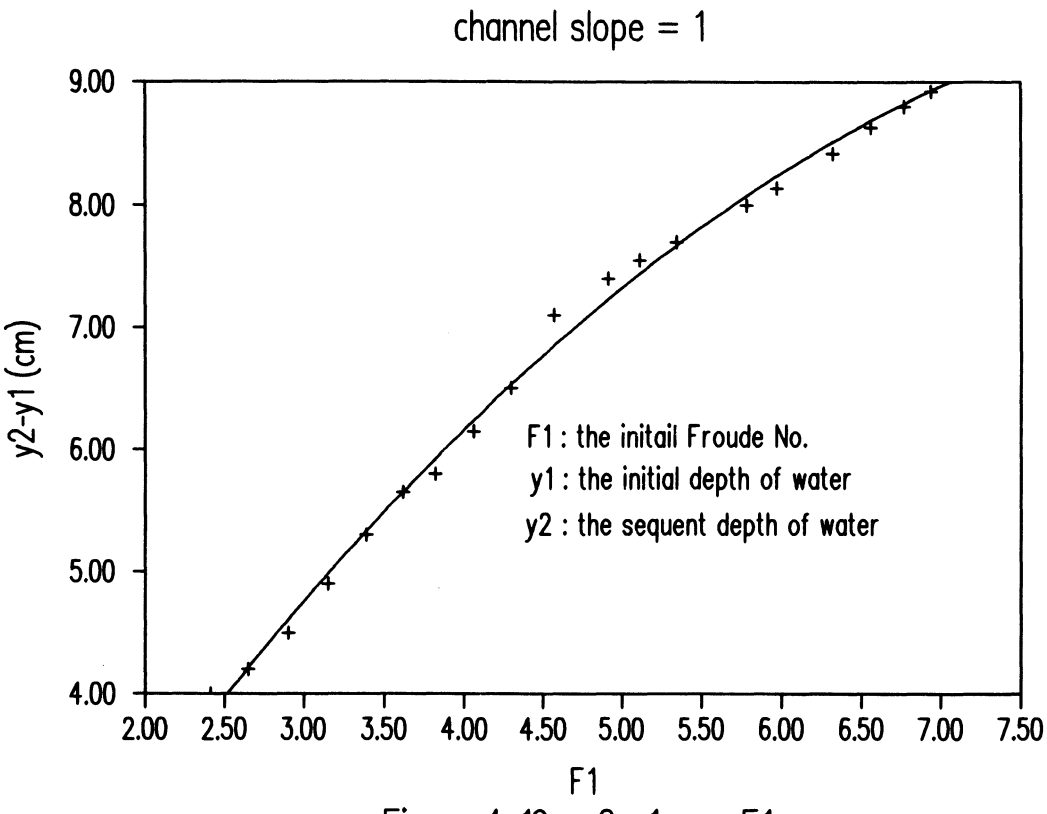

Figure 4-19 : y2-y1 vs F1

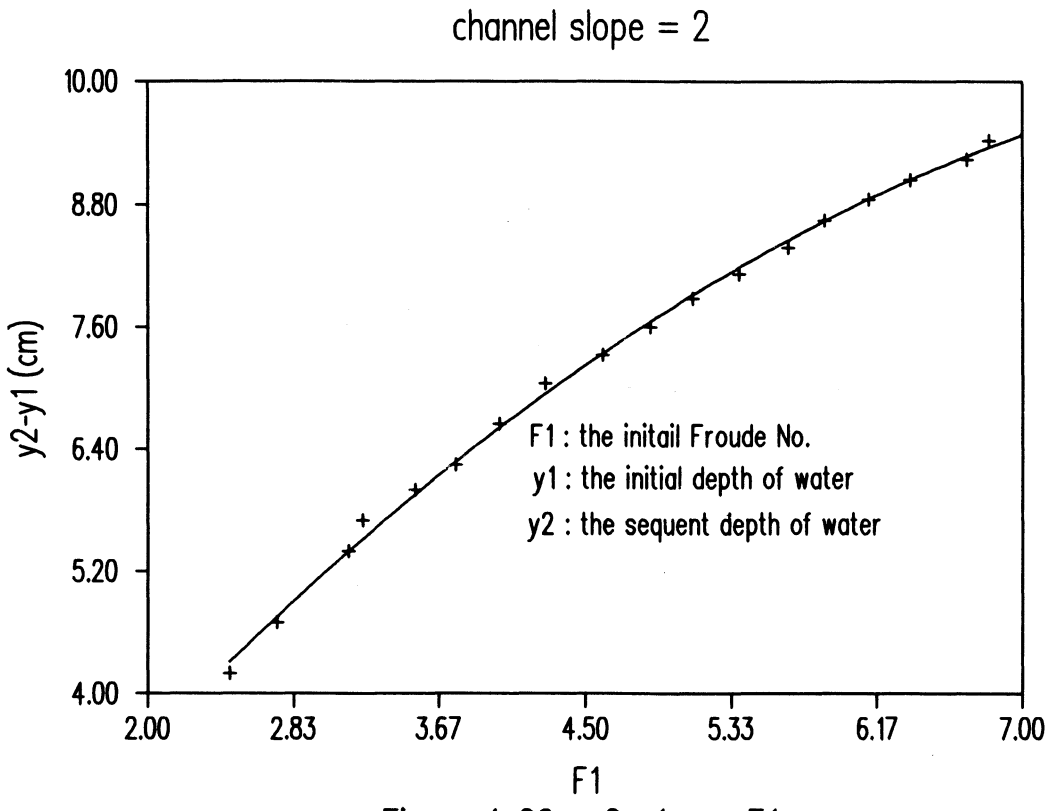

Figure 4-20 : y2-y1 vs F1

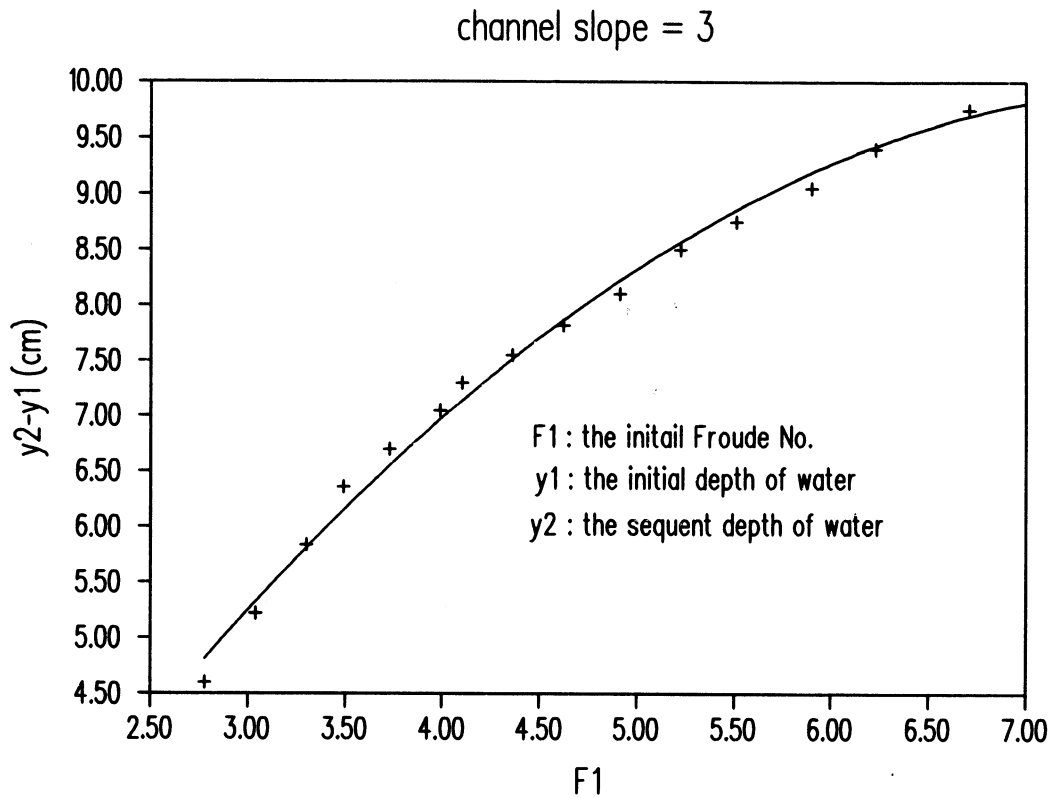

Figure 4-21 : y2-y1 vs F1

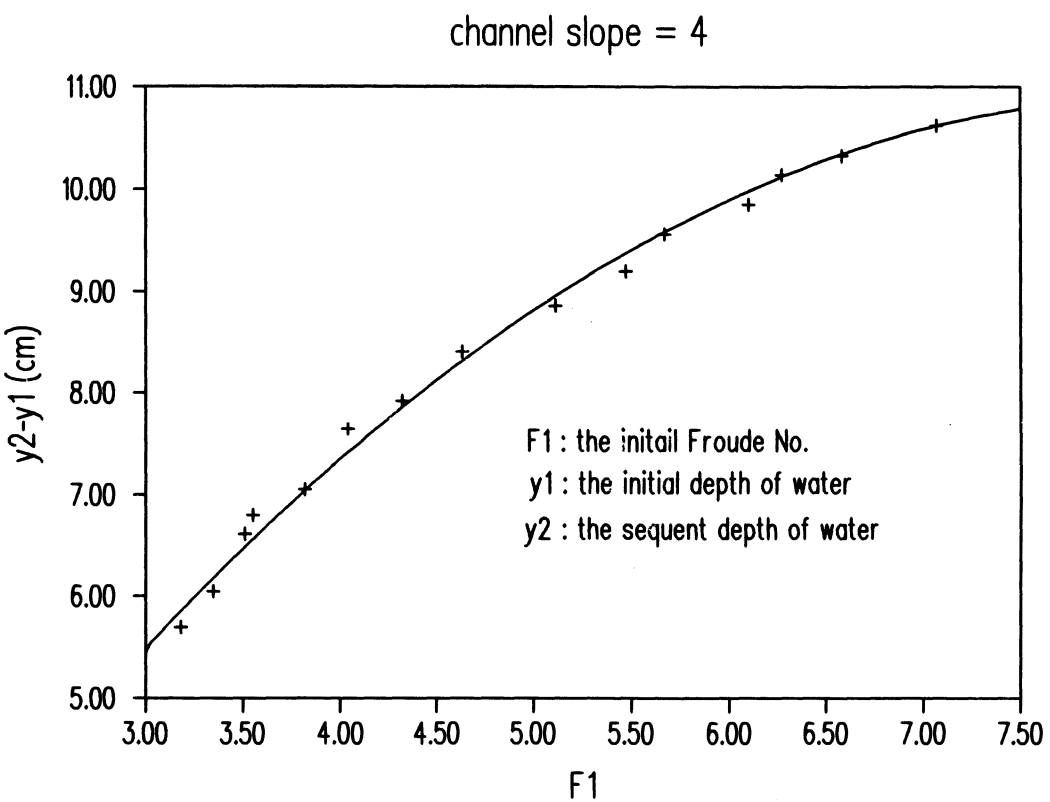

Figure 4-22 : y2-y1 vs F1

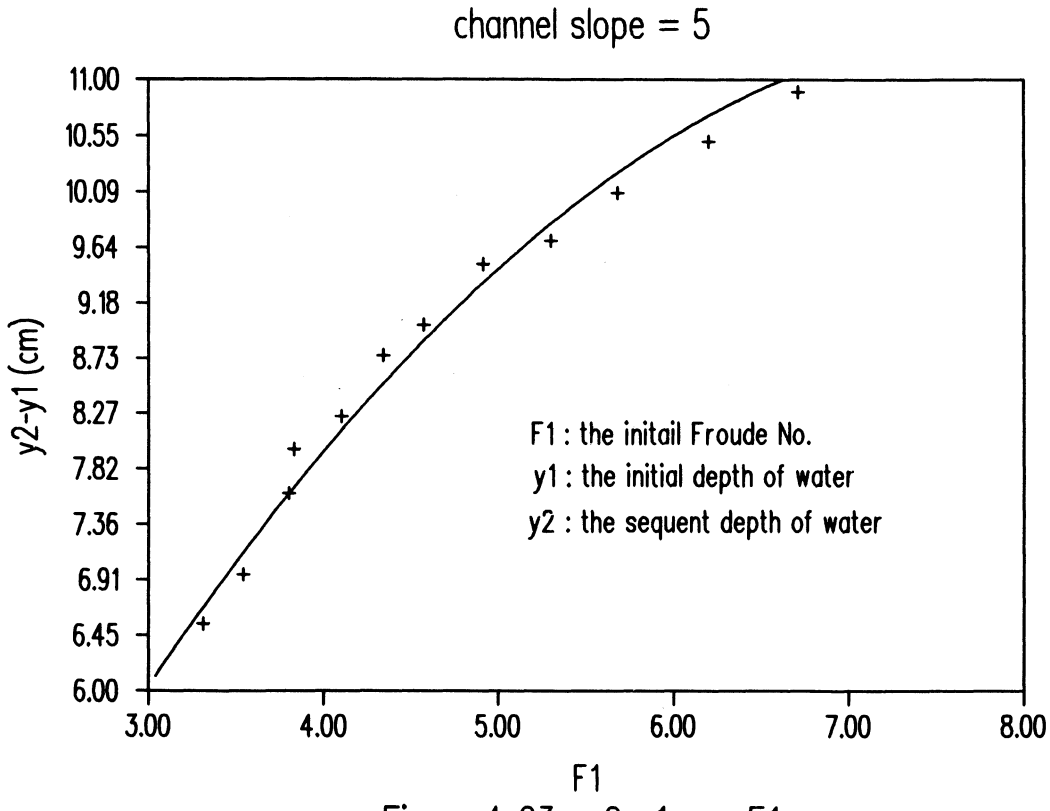

Figure 4-23 : y2-y1 vs F1

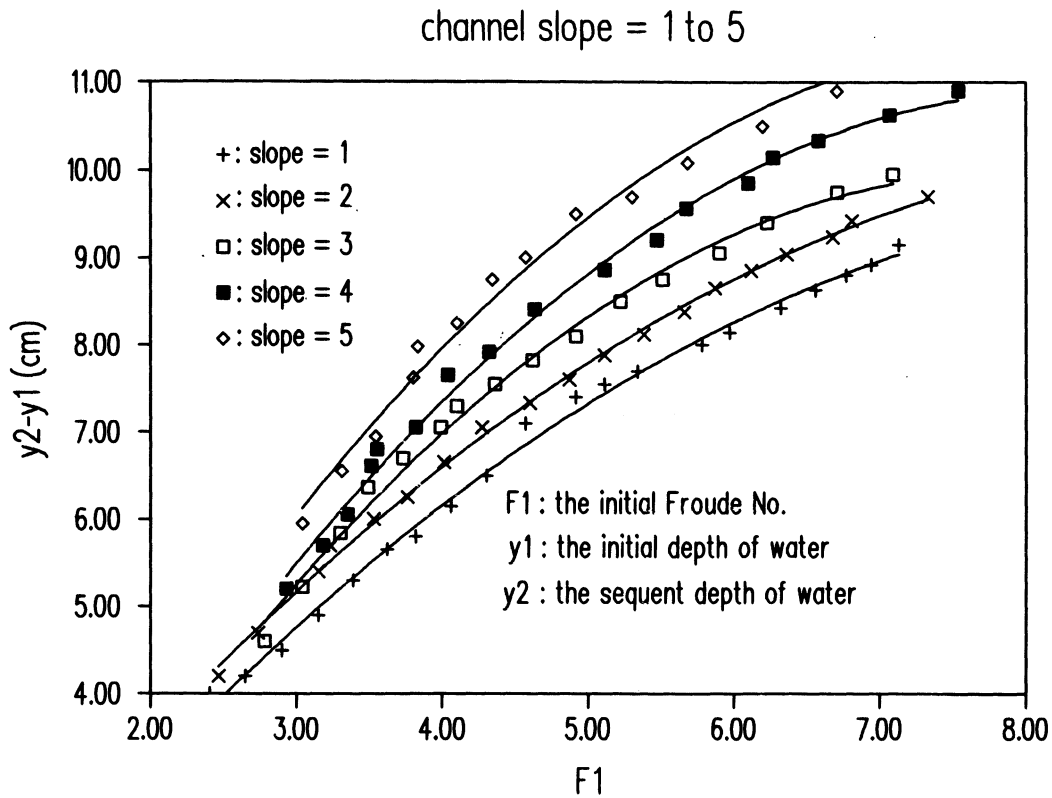

Figure 4-24 : y2-y1 vs F1

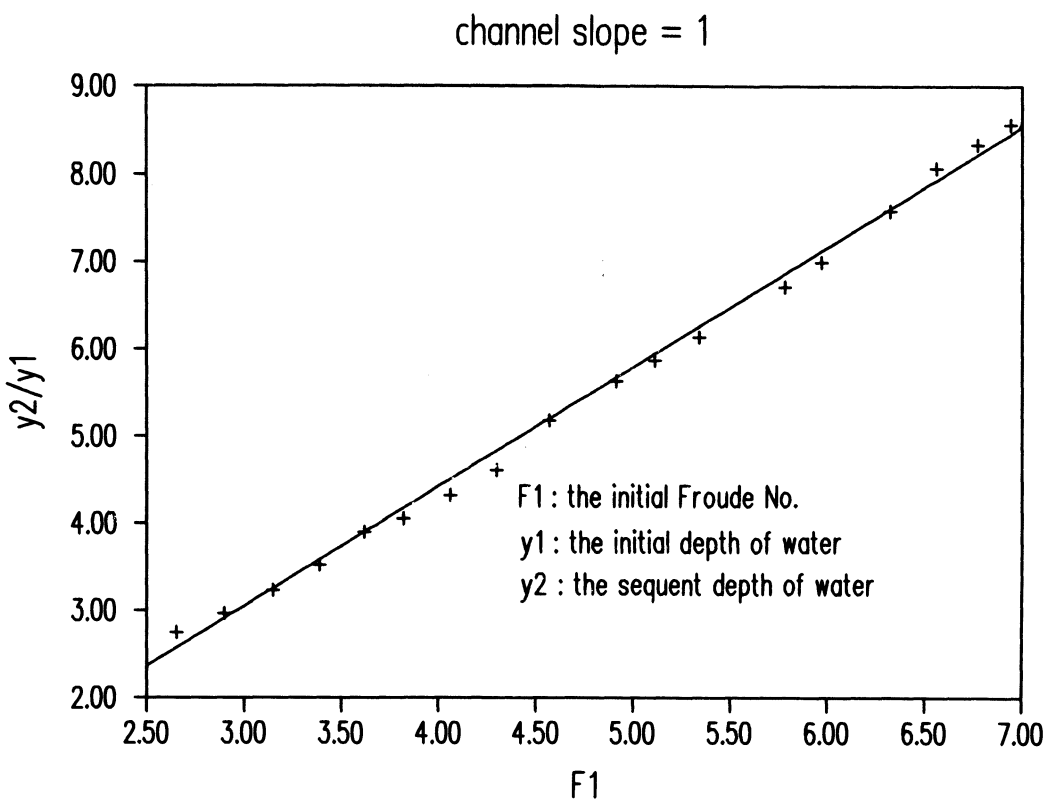

Figure 4-25 : y2/y1 vs F1

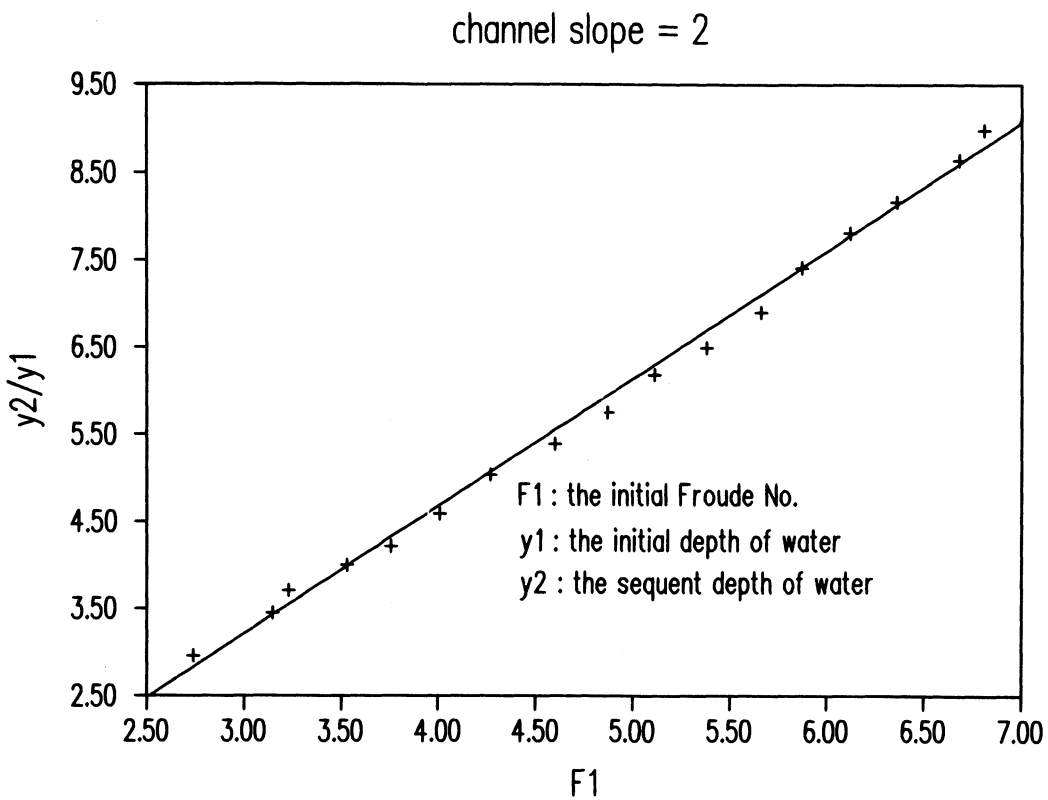

Figure 4-26 : y2/y1 vs F1

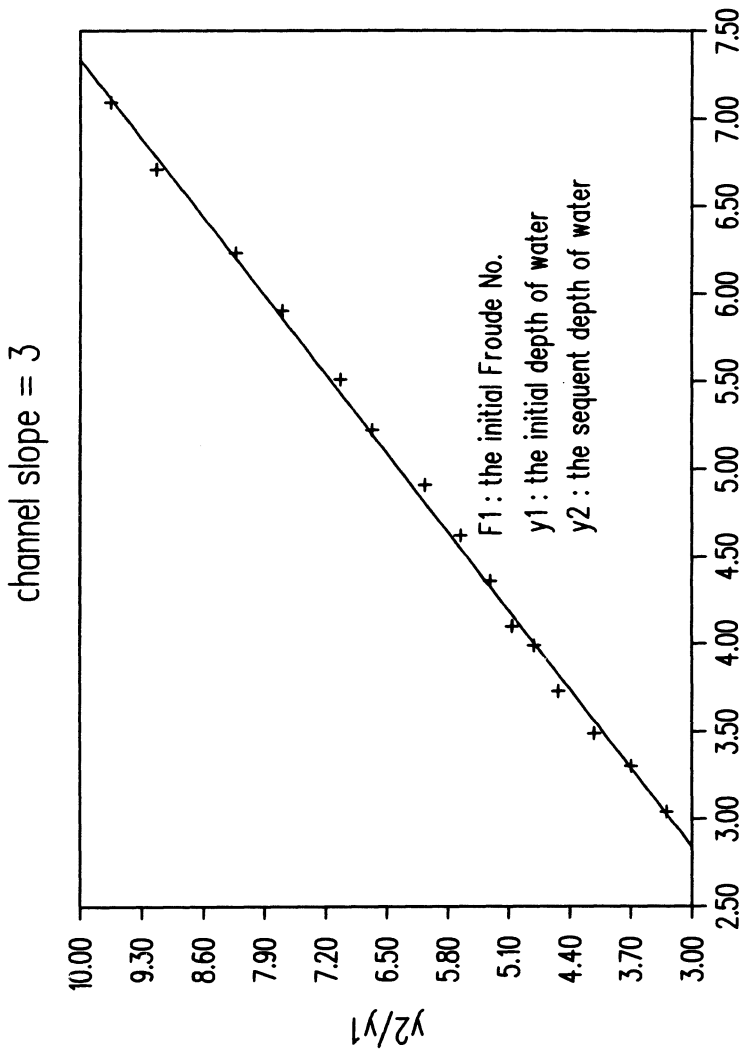

Figure 4-27 : y2/y1 vs F1

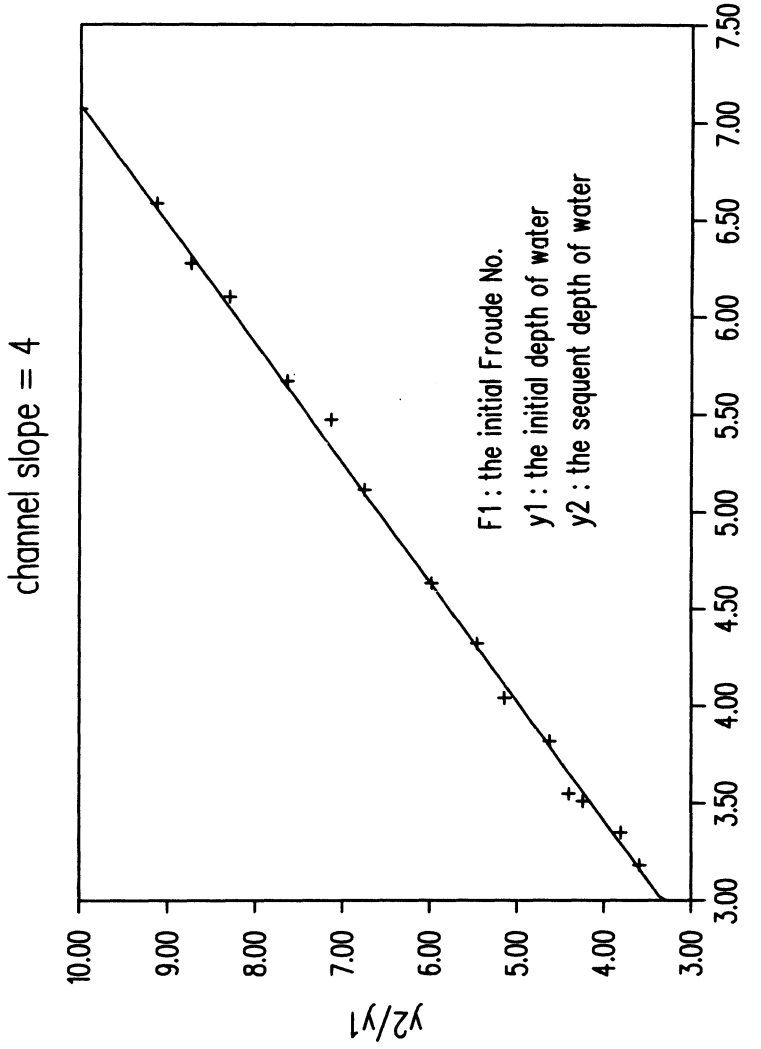

Figure 4-28 : y2/y1 vs F1

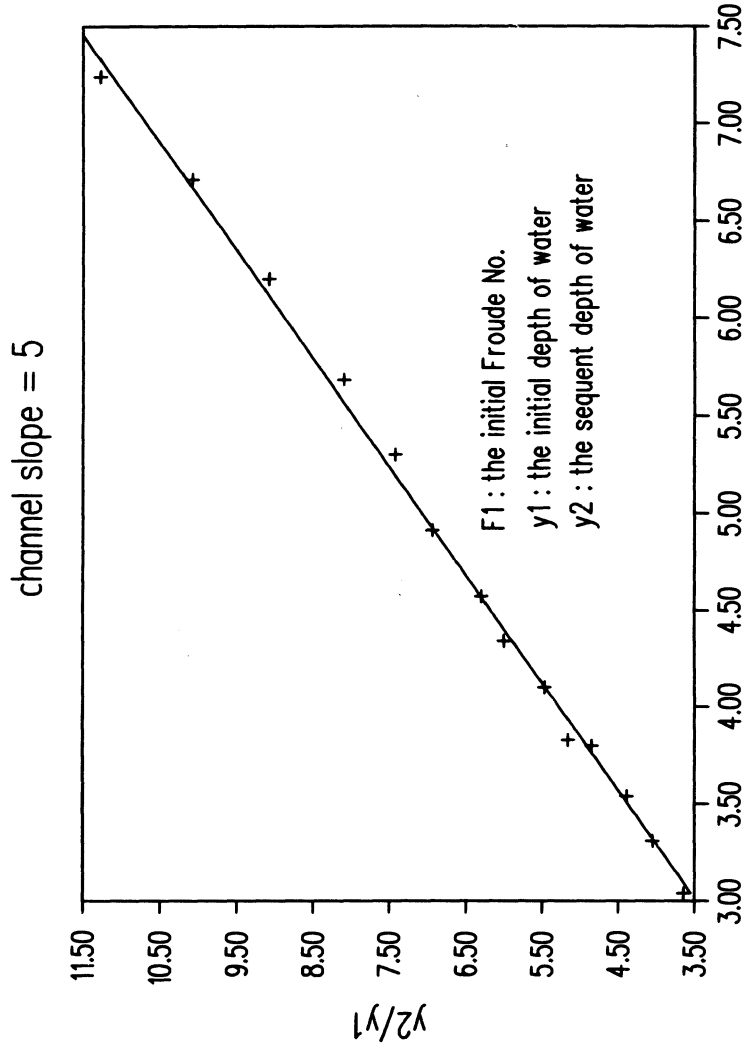

Figure 4-29 : y2/y1 vs F1

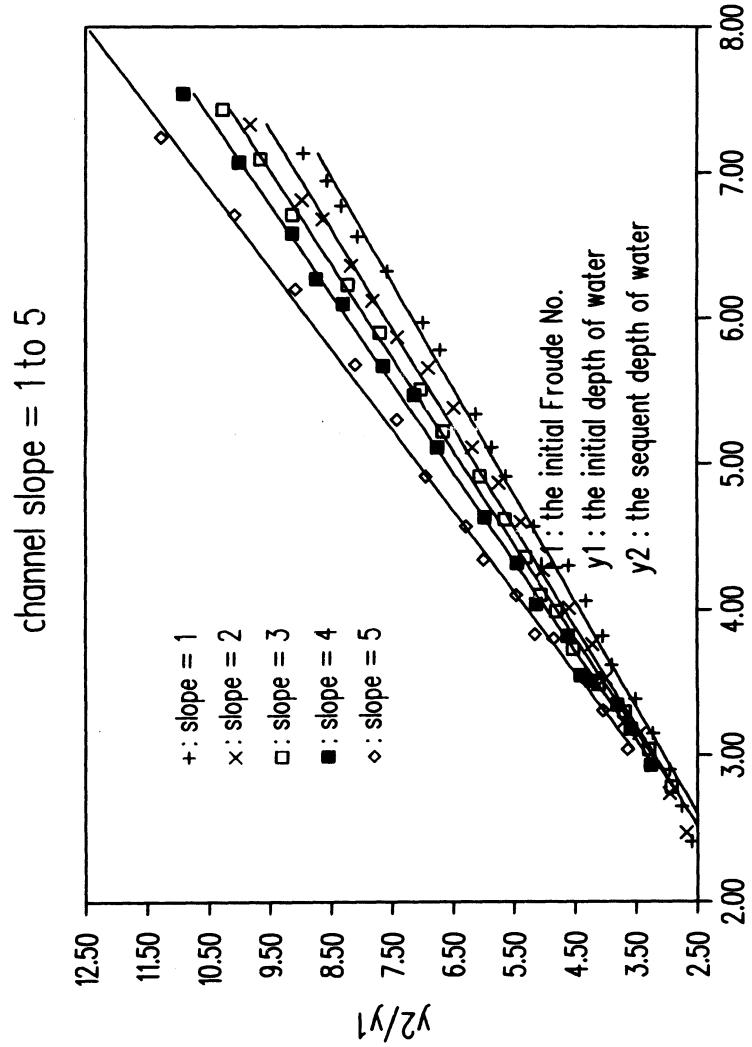

Figure 4-30 : y2/y1 vs F1

CHAPTER V. CONCLUSIONS AND RECOMMENDATIONS

A hydraulic jump is generally used to dissipate high kinetic energy of flow to protect man-made structures such as spillways, drop structures, outlet works, and sluice gates or natural channel banks below spillways. A hydraulic jump offers a perfect location for chemical mixing right before the jump. It enhances the tailwater level to reduce the flow velocity, to stabilize the downstream apron, and to recharge the ground water. Most of previous studies on hydraulic jump have relied on model tests. This study discusses the experimental results of hydraulic jump and introduces their uses in the HEC-2 flow routing for possible determination of hydraulic jump location.

There is a limit of the scales between the models and the prototypes. Generally, the maximum scale is 1:10 and the minimum scale is 1:70 . If the model size is too small some additional equipments such as baffle, piers, and gate become very small; therefore, any change of the shape or location will affect the accuracy of the similitude (Elevatorski,1959). The model test and the HEC-2 flow routing for the corresponding prototype in this study are developed following these rules. The scale is of the experiment 1:65 and the following conclusions are made based on this study.

1. The results of jump length ratio, L_j/y_2 or L_j/y_1, in terms of Froude number, F_1, provide valuable information to estimate lengths of hydraulic jumps at varied channel bed slopes. Furthermore, L_j/y_1 has a linear relation with respect to F_1 while L_j/y_2 does not.

2. Experimental results of the study conclude that the estimation of sequent depth for a hydraulic jump has to take the channel bed slope into account if the bed slope is greater than 3°.

3. The jump height as defined in this study has been developed in relation to the corresponding Froude number F_1. These developed plots can be used for stilling basin designs with regard to their heights.

4. The plots of L_j/y_2 vs. F_1 can be incorporated for locating the toe of a hydraulic jump when the heel of the hydraulic jump is determined in the HEC-2 flow routing.

5. Results of this study show that y_2/y_1 and F_1 have linear relation and can be used to estimate the sequent depth, y_2, for given upstream conditions, i.e, y_1 and F_1. By the procedure developed in this study, y_2 is used in the HEC-2 flow routing to locate the heel of hydraulic jump.

In practical engineering, a hydraulic designer must overcome technical and economic problems in designing hydraulic jump related structures. The following rules are recommended:

1. Arranging the channel to give the greatest economy and perform all functions properly are the important factors in building a sloping hydraulic channel.

2. Ensure a hydraulic jump to be formed within the stilling basin for the maximum tailwater and discharge, and ensure the energy dissipation is sufficient while the stilling basin is not in full capacity.

3. If the economy condition is the first priority, the length of hydraulic jump may not totally confined within the stilling basin. The average length of the apron is 60% of the jump length for the maximum discharge, when the downstream riverbed conditions are good. On the other hand, if the downstream riverbed conditions are not good, such as a loose bed, the whole jump length should be formed within the stilling basin.

4. A solid triangular sill can be arranged at the end of the basin apron to lift the water and reduce the scour from the leaving flow.

5. When the Froude number ranges between 4.5 and 9 the tailwater depth is lowered by 5% of the sequent water depth making it equal to $0.95y_2$. When the Forude number is greater than 15 the tailwater recommended is $1.1y_2$. When the Froude number falls between 2 to 4.5 or 9 to 15 a tailwater depth equal to y_2 is recommended (Elevatorski, 1959).

BIBLIOGRAPHY

1. Adam, M.A., and Ruff, F.J., "Characteristics of B-Jump with Different Toe Locations", Journal of Hydraulic Engineering, ASCE, vol. 119, No. 8, pp. 939-948, 1993.

2. Argyropoulos, P.A., "General Solution of The Hydraulic Jump in Sloping Channels", Journal of Hydraulic Division, ASCE, vol. 88, No.4, pp. 61-75, 1962.

3. Bakheteff, B.A., Hydraulic of Open Channels, McGraw, New York, NY, 1932.

4. Bhowmik, N.G., "Stilling Basin Design for Low Froude Number", Journal of Hydraulic Division, ASCE, vol. 101, No.7, pp. 901-915, 1975.

5. Bowers, C.E., and Tsia F.Y., Fluctuating Pressures in Spillway Stilling Basins[a]", Journal of Hydraulic Division, ASCE, vol. 95, No. 6, pp. 2071-2079, 1969.

6. Bradley, J.N., and Peterka, A.J.,"The Hydraulic Design of Stilling Basins:Hydraulic Jumps on A Horizontal Apron(Basin I)", Journal of Hydraulic Division, ASCE, vol. 83, No. 5, pp. 1041-1-1042, 1957.

7. Bradley, J.N., and Peterka, A.J.,"The Hydraulic Design of Stilling Basins:High Dams, Earth Dams, and Large Canal Structures (Basin II)", Journal of Hydraulic Division, ASCE, vol. 83 , No. 5, pp. 1042-1-1043, 1957.

8. Brow, F.R., Cavitation in Hydraulic Structures: Problems Created by Cavitation Phenomena[a]", Journal of Hydraulic Division, ASCE, vol. 89, No. 1, pp. 99-115, 1957.

9. Cassidy, J.J., "Design Spillway Cresets for High-Head Operation", Journal of Hydraulic Division, ASCE, vol. 96, No.3, pp. 745-754, 1970.

10. Chamberlain, A.R., Jabara, M.A., Murhpy, T.E., and Berryhill, R.H., "Energy Dissipators for Spillways and Outlet Works", Journal of Hydraulic Division, ASCE, vol. 90, No.1, pp. 121-147, 1964.

11. Chang, T.J., "Studies of Hydraulic Jump by The Flow Routine", Hydraulic Engineering Proceeding of the 1988 National Conference, ASCE, pp. 1003-1012, 1988.

12. Chow, V.T., Open-Channel Hydraulics, McGraw, New York, NY, 1959.

13. Elevatorski, E.A., Hydraulic Energy Dissipators, McGraw, New York, NY, 1959.

14. Farhoudi, J., and Narayanan, R., "Forces on Slab Beneath Hycraulic Jump", Journal of Hydraulic Engineering, ASCE, vol.117, No. 1, pp. 64-82, 1991.

15. French, R.H., Open-Channel Hydraulics, McGraw-Hill, New York, NY, 1985.

16. Garg, S.P., and Sharma, H.R., "Efficiency of Hydraulic Jump", Journal of Hydraulic Division, ASCE, vol. 97, No.3, pp. 409-420, 1971.

17. Gharangik, A.M., and Chaudhry, M.H., " Numerical Simulation of Hydraulic Jump", Journal of Hydraulic Engineering, ASCE, vol.117, No. 9, pp. 1195-1211, 1991.

18. Hager, W.H., "Discusion of Design of Hydraulic Jump Chambers", Journal of Irrigation and Drainage Engineering, ASCE, vol.117, No. 6, pp. 979-982, 1991.

19. Hager, W.H., "Impact Hydraulic jump", Journal of Hydraulic Engineering, ASCE, vol.120, No. 5, pp. 633-637, 1994.

20. Hager, W.H., "Classical Hydraulic Jump: Free Surface Profile", Canadian Journal of Civil Engineering, vol. 20(3), June, pp. 536-539, 1993.

21. Hager, W.H., "Disscussion of Force on Slab Beneath Hydraulic Jump", Journal of Hydraulic Engineering, ASCE, vol.118, No. 4, pp. 666-668, 1992.

22. Hager, W.H., "Bjump at Abrupt Channel Drops", Journal of Hydraulic Engineering, ASCE, vol.111, No. 5, pp. 861-866, 1985.

23. Hager, W.H., Basler, B., and Wanoschek, R., "Incipient Jump Condition for Ventilated Sill Flow", Journal of Hydraulic Engineering, ASCE, vol.112, No. 10, pp. 953- 963, 1986.

24. Hari, V.M., "Disscussion of Spercritical Flow Over Sills at Incipient Jump Conditions", Journal of Hydraulic Division, ASCE, vol. 99, No.8, pp. 1278-1279, 1973.

25. Hederson, F.M., Open Channel Flow, Macmillan, New York, NY, 1966.

26. Hoyt, J.W., and Sellin, H.J., "Hydraulic Jump as "mixing Layer" ", Juornal of Hydraulic Engineering, ASCE, vol.115, No. 12, pp. 1607-1614, 1989.

27. Hughes, W.C., and Flack, J.E., "Hydraulic Jump Properties Over a Rough Bed", Juornal of Hydraulic Engineering, ASCE, vol.110, No. 12, pp. 1755-1771, 1984.

28. Jain, S.C. "Nonuique Water-Surface Profiles in Open Channels", Journal of Hydraulic Engineering, ASCE, vol.119, No. 12, pp. 1427-1434, 1993.

29. Jeppson, R.w., "Graphical Solution to Hydraulic jump", Journal of Hydraulic Division, ASCE, vol. 96, No.1, pp. 1041-1-1042, 1970.

30. Jones, J.O., Introducetion to Hydraulic and Fluid Mechanics, Harper & Brothwe, New York, NY, 1953.

31. Karki, K.S., "Supercritical Flow Over Sills", Jump Condtions", Journal of Hydraulic Division, ASCE, vol. 102, No.10, pp. 1449-1459, 1976.

32. Karki, K.S., Chander, S., and Malhotra, R., "Supercritical Flow over Sills at Incipient Jump Condtions", Journal of Hydraulic Division, ASCE, vol. 98, No.10, pp. 1753-1764, 1972.

33. Keller, R.J., and Rastogi, A.K., "Design Chart for Prediciting Critical Point on Spillways",Journal of Hydraulic Division, ASCE, vol. 103, No.12, pp. 1417-1429, 1977.

34. Khader, M.H.A., and Rao, H.S., "Discussion of Pattern of Potential Flow in A Overfall", Journal of Hydraulic Division, ASCE, vol. 96, No.11, pp. 2397-2398, 1970.

35. King, H.W., and Braer, E.F., Handbook of Hydraulic for the Solution of Hydraulic and Fluid-Flow Promblems, McGraw, New York, NY, 1963.

36. Larock, B.E., "Gravity-Affected Flow From Planar Sluice Gates", Journal of Hydraulic Division, ASCE, vol. 95, No.4, pp. 1211-1226, 1969.

37. Lawrence, G.A., "Steady Flow Over An Obstacle", Journal of Hydraulic Engineering, ASCE, vol.113, No. 8, pp. 981-991, 1987.

38. Leutheusser, H.J., and Kartha, V.C., "Effects of Inflow Condition on Hjdraulic Jump", Journal of Hydraulic Division, ASCE, vol. 98, No.8, pp.1367-1385, 1972.

39. Linsley, R.K., and Franzini, J.B., Water-Resources Engineering, McGraw, New York, NY, 1972.

40. Martin, C.S., and DeFazio, F.G., "Open-channel Surge Simulation by Digital Computer", Journal of Hydraulic Division, ASCE, vol. 95, No.6, pp.2049-2070, 1969.

41. McCorquodale, J.A., "Supercricial Flow Over Sills", Journal of Hydraulic Division, ASCE, vol. 98, No. 4, pp. 667-679, 1972.

42. McCorquodale, J.A., and Khalifa, A., "Internal Flow in Hydraulic Jumps", Journal of Hydraulic Engineering, ASCE, vol. 109, No.5, pp. 684-701, 1983.

43. McCorquodale, J.A., and Khalifa, A., "Submerged Radial Hydraulic Jump", Journal of Hydraulic Division, ASCE, vol. 106, No.3, pp. 355-367, 1980.

44. Mohamed, H.S., "Effect of Roughened-Bed Stilling Basin on Length of Rectangular Hydraulic Jump", Journal of Hydraulic Engineering, ASCE, vol. 117, No.1, pp. 83-93, 1991.

45. Molinas, A., and Yang, C.T., "Generalized Water Surface Profile Computations", Journal of Hydraulic Engineering, ASCE, vol.111, No. 3, pp. 381-397, 1985.

46. Narayanan, R., "Wall Jet Analogy to Hydraulic Jump", Journal of Hydraulic Division, ASCE, vol. 101, No.3, pp. 347-359, 1975.

47. Narayanan, R., "Cavitation Induces by Turbulence in Stilling Basin", Journal of Hydraulic Engineering, ASCE, vol.106, No. 4, pp. 617-619, 1980.

48. Narayanan, R., and Schizas, L., "Force on Sill of Forced Jump", Journal of the Hydraulic Division, ASCE, vol. 106, No. 7, pp. 1159-1171, 1980.

49. Narayanan, R., and Schizas, L.S.. "Force Fluctuations on Sill of Hydraulic Jump", Journal of Hydraulic Division, ASCE, vol. 106, No. 4, pp. 589-599, 1980.

50. Ohtsu, I., and Yasuda, Y., "Hydraulic Jump in Sloping Channels", Journal of Hydraulic Engineering, ASCE, vol.117, No. 7, pp. 905-921, 1991.

51. Ohtsu, I., and Yasuda, Y., "Characteristics of Supercritical Flow Below Sluice Gate", Journal of Hydraulic Engineering, ASCE, vol.120, No. 3, pp. 332-346, 1994.

52. Pillai, N.N., Goel,A., and Dubey, A.K., "Hydraulic Jump Type Stilling Basin for Low Froude Number", Journal of Hydraulic Engineering, ASCE, vol.115, No. 7, pp. 989-994, 1981.

53. Rajaratnam, N., "Free Flow Immediately Below Sluice Gates", Journal of Hydraulic Division, ASCE, vol. 103, No. 4, pp. 345-351, 1977.

54. Rajaratnam, N., and Subramanya, K., "Profile fo The Hydraulic Jump", Journal of Hydraulic Division, ASCE, vol. 94, No. 3, pp. 663-673, 1968.

55. Rajaratnam, N., and Murahari, V., "Flow Characteristics of Sloping Channel Jumps", Journal of Hydraulic Division, ASCE, vol. 100, No. 6, pp. 731-740, 1974.

56. Rand, W., "Flow Over A Vertical Sill in An Open Channel", Journal of Hydraulic Division, ASCE, vol. 91, No. 4, pp. 97-121, 1965.

57. Rao, N.S.G., and Rajaratnam, N., "The Submerged Hydraulic Jump", Journal of Hydraulic Division, ASCE, vol. 89, No. 1, pp. 139-162, 1963.

58. Rhone, T.J., "Baffled Apron As Spillway Energy Dissipator", Journal of Hydraulic Division, ASCE, vol. 103, No. 12, pp. 1391-1401, 1977.

59. Robinson, D.I., and McGhee, T.J., "Computer Modeling of Side-Flow Weirs", Journal of Irrigation and Drainage Engineering, ASCE, vol. 119, No. 6, pp. 989-1005,1993.

60. Rose, H., Fluid Mechanics for Hydraulic engineers, McGraw, New York, NY, 1938.

61. Sarma, K.V.N., and Syamala, P., "Supercritical Flow in Smooth Open Channel", Journal of Hydraulic Engineering, ASCE, vol. 117, No. 1, pp.54-63, 1991.

62. Sarikell, S.F.K., and Simon, A.L., "Design of the Hydraulic Jump Chambers", Journal of Irrigation and Drainage Engineering, ASCE, vol. 116, No. 2, pp. 143-153, 1990.

64. Sharp, J.J., "Observations on Hydraulic Jumps at Rounded Step", Journal of Hydraulic Division, ASCE, vol. 100, No. 6, pp.787-795, 1974.

65. Silvester, R., "Hydraulic Jump in all Shapes of Horizontal Channels", Journal of Hydraulic Division, ASCE, vol. 90, No. 1, pp.23-55, 1964.

66. Toso, J.W., and Bower, C.E., "Extreme Pressures in Hydraulic-Jump Stilling Basins", Journal of Hydraulic Engineering, ASCE, vol. 114, No. 8, pp.829-843, 1988.

67. Wilson, E.H., and Turner, A.A., "Boundary Layer Effects on Hydraulic Jump Location", Journal of Hydraulic Division, ASCE, vol. 98, No. 7, pp.1127-1142, 1972.

Table A-1: Examples and results of HEC-2 flow routing

	Channel cross section (m)	Water depth HEC-2 computation (m)
	0	7.50
1. Flow discharge $Q = 164$ (cms)	70	6.17
2. Channel bed slope $\theta = 1^{\circ}$	100	5.64
3. Initial Froude No. $F_1 = 5.78$	200	3.00
	300	3.01
5. Tailwater depth $y_t = 7.50$ (m)	400	3.01
6. Sequent depth model test $y_{2ep} = 6.17$ (m)	500	3.01
	600	3.01
	700	3.01
	800	3.01
	900	3.01
	1000	3.01

Table A-2: Example and results of HEC-2 flow routing

	Channel cross section (m)	Water depth HEC-2 computation (m)
	0	8.00
1. Flow discharge $Q = 164$ (cms)	50	6.10
2. Channel bed slope $\theta = 2°$	52	6.04
3. Initial Froude No. $F_1 = 4.87$	100	3.80
	200	3.00
5. Tailwater depth $y_t = 8.00$ (m)	300	3.01
6. Sequent depth model test $y_{2ep} = 6.04$ (m)	400	3.01
	500	3.01
	600	3.01
	700	3.01
	800	3.01
	900	3.01
	1000	3.01

Table A-3: Example and results of HEC-2 flow routing

	Channel cross section (m)	Water depth HEC-2 computation (m)
	0	9.00
1. Flow discharge $Q = 164$ (cms)	46	6.40
2. Channel bed slope $\theta = 3^{\circ}$	48	6.36
3. Initial Froude No. $F_1 = 4.91$	100	3.01
	200	3.00
5. Tailwater depth $y_t = 9.00$ (m)	300	3.01
6. Sequent depth model test $y_{2ep} = 6.36$ (m)	400	3.01
	500	3.01
	600	3.01
	700	3.01
	800	3.01
	900	3.01
	1000	3.01

Table A-4: Example and results of HEC-2 flow routing

	Channel cross section (m)	Water depth HEC-2 computation (m)
	0	9.80
1. Flow discharge $Q = 164$ (cms)	40	6.85
2. Channel bed slope $\theta = 4^{\circ}$	42	6.71
3. Initial Froude No. $F_1 = 5.11$	100	3.00
	200	3.01
5. Tailwater depth $y_t = 9.8$ (m)	300	3.01
6. Sequent depth model test $y_{2ep} = 6.85$ (m)	400	3.01
	500	3.01
	600	3.01
	700	3.01
	800	3.01
	900	3.01
	1000	3.01

Table A-5: Example and results of HEC-2 flow routing

	Channel cross section (m)	Water depth HEC-2 computation (m)
	0	11.00
1. Flow discharge $Q = 164$ (cms)	40	7.36
2. Channel bed slope $\theta = 5^{\circ}$	100	3.0
3. Initial Froude No. $F_1 = 5.30$	200	3.01
	300	3.01
5. Tailwater depth $y_t = 11.0$ (m)	400	3.01
6. Sequent depth model test $y_{2ep} = 7.35$ (m)	500	3.01
	600	3.01
	700	3.01
	800	3.01
	900	3.01
	1000	3.01